



Ice core evidence for a recent increase in snow accumulation in coastal Dronning Maud Land, East Antarctica

Morgane Philippe¹, Jean-Louis Tison¹, Karen Fjøsne¹, Bryn Hubbard², Helle A. Kjær³, Jan T. M. Lenaerts⁴, Simon G. Sheldon³, Kevin De Bondt⁵, Philippe Claeys⁵, Frank Pattyn¹

5 ¹Laboratoire de Glaciologie, Département des Géosciences, Environnement et Société, Université Libre de Bruxelles, BE-1050 Brussels, Belgium

²Centre for Glaciology, Department of Geography and Earth Sciences, Aberystwyth University SY23 3DB, United Kingdom

10 ³Centre for ice and climate, Niels Bohr Institute, University of Copenhagen, Juliane Maries Vej 30, 2100, Copenhagen, Denmark

⁴Institute for Marine and Atmospheric research Utrecht, Utrecht University, Princetonplein 5, 3584 CC Utrecht, Netherlands

⁵Department of Analytical Environmental and Geo-Chemistry, Vrije Universiteit Brussel, Pleinlaan 2, BE-1050 Brussels, Belgium

15 *Correspondence to:* M. Philippe (mophilip@ulb.ac.be)

Abstract. Ice cores provide temporal records of snow accumulation, a crucial component of Antarctic mass balance. Coastal areas are particularly under-represented in such records, despite their relatively high and sensitive accumulation rates. Here we present records from a 120 m ice core drilled on Derwael Ice Rise, coastal Dronning Maud Land (DML), East Antarctica in 2012. We date the ice core bottom back to 1745 ± 2 AD. $\delta^{18}\text{O}$ and δD stratigraphy is supplemented by discontinuous major ion profiles, and verified independently by electrical conductivity measurements (ECM) to detect volcanic horizons. The resulting annual layer history is combined with the core density profile to calculate accumulation history, corrected for the influence of ice deformation. The mean long-term accumulation is 0.425 ± 0.035 m water equivalent (w.e.) a^{-1} (average corrected value). Reconstructed annual accumulation rates show an increase from 1955 onward to a mean value of 0.61 ± 0.02 m w.e. a^{-1} between 1955 and 2012. This trend is compared to other reported accumulation data in Antarctica, generally showing a high spatial variability. Output of the fully coupled Community Earth System Model demonstrates that sea ice and atmospheric patterns largely explain the accumulation variability. This is the first record from a coastal ice core in East Antarctica showing a steady increase during the 20th and 21st centuries, thereby supporting modelling predictions.



1 Introduction

In a changing climate, it is important to know the Surface Mass Balance (SMB) of Earth's ice sheets as it is an essential component of their total mass balance, directly affecting sea level (Rignot et al., 2011). The average rate of Antarctic contribution to sea level rise is estimated to have increased from 0.08 [−0.10 to 0.27] mm a^{−1} for 5 1992–2001 to 0.40 [0.20 to 0.61] mm a^{−1} for 2002–2011 mainly due to rising ice discharge from coastal West Antarctica (Vaughan et al., 2013).

This increase in ice loss could be partly balanced by a warming-related increase in precipitation in East Antarctica (e.g. Polvani et al., 2011; Krinner et al., 2007). There is consistent evidence that past Antarctic snow accumulation rates were positively correlated with past air temperature, as recently shown by Frieler et al. (2015) 10 using ice core data and modelling. Similarly, satellite radar and laser altimetry suggest mass gain in East Antarctica (Shepherd et al., 2012), in particular in DML, which has experienced several high-accumulation years since 2009 (Boening et al., 2012; Lenaerts et al., 2013). However, although recent regional atmospheric climate models indicate higher accumulation along the coastal sectors than in previous estimates, they show no long-term trend in the total accumulation over the continent during the past few decades (Monaghan et al., 2006; van 15 den Broeke et al., 2006; Bromwich et al., 2011; Lenaerts et al., 2012).

Ice cores provide temporal records of snow accumulation. These are essential to calibrate internal reflection horizons in radio-echo sounding records (e.g. Fujita et al., 2011; Kingslake et al., 2014), to force ice sheet flow and dating models (e.g. Parenin et al., 2007) and to evaluate regional climate models (e.g. Lenaerts et al., 2014). However, records of accumulation are still scarce relative to the size of Antarctica. Whilst the majority lack a 20 significant trend in snow accumulation over the last century (e.g. Nishio et al., 2002), some do show an increase (e.g. Karlof et al., 2005), and others show a decrease (e.g. Kaczmarska et al., 2004). Frezzotti et al. (2013) compiled surface accumulation records for the whole of Antarctica and Altnau et al. (2015) for Dronning Maud Land (DML). Both authors concluded that the trends are insignificant.

However, there is still a clear need for data from the coastal areas of East Antarctica (ISMASS Committee, 2004; 25 van de Berg et al., 2006; Magand et al, 2007), where very few studies have focused on ice cores, and few of those have spanned more than 20 years. Coastal regions allow higher temporal resolution as accumulation rates generally decrease with both altitude and distance from the coast (Frezzotti et al., 2005). Ice rises are ideal locations for paleoclimate studies (Matsuoka et al., 2015) as they are undisturbed by up-stream topography, since lateral flow is almost negligible. Melt events are also likely to be much less frequent than on ice shelves 30 (Hubbard et al., 2013).



In this paper we report on continuous ice $\delta^{18}\text{O}$ and δD measurements (5-10 cm resolution) along a 120 m core drilled on Derwael Ice Rise ($70^{\circ}14'44.88''$ S, $26^{\circ}20'5.64''$ E), in coastal DML. This record is complemented by major ions profiles to improve the resolution of the seasonal cycles wherever necessary. Dating is checked independently using volcanic horizons detected from continuous electrical conductivity measurements (ECM) along the core (Hammer et al., 1994). After correcting for dynamic vertical thinning, we derive annual accumulation, and average accumulation and trends over the last 267 years, i.e. across the Anthropocene transition. These are compared to other reported trends in Antarctica including DML over the last 20 and 50 years.

2 Field site and methods

10 2.1 Field site

The study site is located in coastal DML, East Antarctica. A 120 m ice core was drilled in 2012 on the divide of Derwael Ice Rise, named IC12 after the project name IceCon ($70^{\circ}14'44.88''$ S, $26^{\circ}20'5.64''$ E Figure 1), which is 486 m thick and has a local ice flow (Drews et al., 2015). Due to its coastal location, the accumulation rate is high and allows dating by seasonal peak counting. Only a few very thin melt layers are present. A continuous density profile was obtained by calibrating optical televiewer (OPTV; Hubbard et al. 2008) luminosity records in the borehole with discontinuous gravimetric measurements (Hubbard et al., 2013).

2.2 Ice coring

The IC12 ice core was drilled with an Eclipse electromechanical ice corer in a dry borehole. The mean length of the core sections recovered after each run was 0.77 and the standard deviation 0.40 m. Immediately after drilling, temperature (Testo 720 probe, inserted in a 4 mm diameter hole drilled to the centre of the core, precision ± 0.1 °C) and length were measured on each core section, which was then wrapped in a PVC bag and stored directly in a refrigerated container at -25 °C, and kept at this temperature until analysis. The core sections were then split lengthwise in two, in a cold room at -20 °C. One half of the core section was used for ECM measurements and then kept as archive, while the other half was sectioned for continuous stable isotope sampling and discontinuous major ion analysis.



2.3 Annual layer counting and dating

2.3.1 Water stable isotopes and major ions

Half of each core section was resampled as a central bar of 30 mm square section with a clean band saw. The outer part of the half-core was melted and stored in 4 ml bottles for $\delta^{18}\text{O}$ and δD measurements, completely
5 filled to prevent contact with air. For major ions measurements, the inner bar was then placed in a Teflon holder and further decontaminated by removing ~2 mm from each face under a class-100 laminar flow hood, using a methanol-cleaned microtome blade. Each 5 cm-long decontaminated section was then covered with a clean PE storage bottle, and the sample cut loose from the bar by hitting it perpendicularly to the bar axis. Blank ice samples prepared from milliQ water were processed before every new core section and analysed for
10 contamination.

Dating was achieved by annual layer counting identified from the stratigraphy of the $\delta^{18}\text{O}$ and δD isotopic composition of H_2O measured (10 cm resolution in the top 80 m and 5 cm resolution below) with a PICARRO L 2130-i Cavity Ring Down Spectrometer (CRDS) (precision, $\sigma = 0.05 \text{‰}$ for $\delta^{18}\text{O}$ and 0.3‰ for δD). The annual layer was identified by the $\delta^{18}\text{O}$ summer maximum value.

15 For sections of unclear isotopic seasonality, major ion analysis (Na^+ , SO_4^- , NO_3^- , Cl^-) was performed with a Dionex-ICS5000 liquid chromatograph. The system has a standard deviation of 2 ppb for Na^+ and SO_4^- , 7 ppb for NO_3^- , and 8 ppb for Cl^- . Non sea-salt sulfate was calculated as $nss\text{SO}_4 = [\text{SO}_4^-]_{\text{tot}} - 0.052 * [\text{Cl}^-]$, following Mulvaney et al. (1992) and represents all SO_4^- not of a marine aerosol origin. The ratio $R_{\text{Na}^+/\text{SO}_4^-}$ was also calculated as an indicator of seasonal SO_4^- production.

20 2.3.2 ECM and volcanic horizons

ECM measurements were made in a cold room at -18°C at the Centre for Ice and Climate, Niels Bohr Institute, University of Copenhagen with a modified version of the Copenhagen ECM described by Hammer (1980). Direct current (1250 V) was applied at the surface of the freshly cut ice and electrical conductivity was measured at a 1 mm resolution. The DC electrical conductivity of the ice, once corrected for temperature, depends
25 principally on its impurity content located at the crystal boundaries (SO_4^- , NO_3^- , Cl^- , etc.) (Hammer, 1980; Hammer et al., 1994). This content varies seasonally and shows longer term maxima associated with sulfate production from volcanic eruptions. ECM can therefore be used both as a relative and an absolute dating tool. ECM data were smoothed with a 301 point wide first-order Savitsky-Golay filter (Savitsky and Golay, 1964). As measurements were principally made in firn, we multiplied the signal by the ratio of the ice density to firn



density following Kjær (2014). Finally, data were normalized by subtracting the mean and dividing by the standard deviation following Karlof et al. (2000). We selected potential volcanic peaks as those above the 2σ threshold, following standard practice (e.g. Kaczmarska et al., 2004).

2.4. Corrections

5 Snow burial not only involves density changes along the vertical, but also involves lateral deformation of the underlying ice. Failure to take the latter process into account would provide an underestimation of reconstructed initial annual layer thickness, and therefore of the accumulation rate, especially within the oldest part of the record. Commonly, three different models are used to represent vertical strain rate evolution with depth: (i) a power-law model (Lliboutry, 1979), (ii) a piece-wise linear model (Dansgaard and Johnsen, 1969) and (iii) a
10 fully linear model (Nye, 1963).

(i) The power-law model requires measurements of the borehole horizontal displacement, which are unfortunately not available. (ii) The piece-wise model assumes a constant vertical strain rate between the surface and a given depth, which in our case is below the zone of interest since the ice core is drilled in the first quarter of the total ice rise thickness (486 m, Drews et al., 2015), and then a quadratic decrease to zero at the ice-bedrock
15 interface. The constant strain-rate in the upper part of the ice sheet can be inferred from the slope of water equivalent (w.e.) annual layer thickness versus depth, also in m w.e., assuming a constant long term snow accumulation (equal to annual layer thickness at the surface, Roberts et al., 2014). (iii) Finally, the Nye model corrects the layer thickness L by assuming ice is incompressible, with a linear decrease from a constant annual layer thickness at the surface to zero at the ice bedrock interface (which implies a constant total ice thickness). In
20 that case, $L_z = L_s (z/H)$, where H is the total ice thickness in m w.e., and subscripts s and z represent the values at the surface and at a height z (in m w.e.) above the bed.

The last two corrections were applied separately and are compared in the results section.

2.5 Community Earth System Model (CESM)

To interpret our ice core derived accumulation record and relate it to the large-scale atmospheric and ocean
25 conditions, we use outputs of the Community Earth System Model (CESM). CESM is a global, fully coupled, CMIP6-generation climate model with an approximate horizontal resolution of 1 degree, and has recently been shown to realistically simulate present-day Antarctic climate and SMB (Lenaerts et al., in press). We use the historical time series of CESM (156 years, 1850-2005) that overlaps with most of the ice core record, and group the 16 single (~10%) years with the highest accumulation and lowest accumulation in that time series. We take



the mean accumulation of the ice covered CESM grid points of the coastal region around the ice core (20-30 degrees East, 69-72 degrees South) as a representative value. For the grouped years of high and low accumulation we take the anomalies (relative to the 1850-2005 mean) in near-surface temperature, sea-ice fraction and surface pressure as parameters to describe the regional ocean and atmosphere conditions
5 corresponding to these extreme years.

3 Results

3.1 Dating

3.1.1 Relative dating (seasonal peak counting)

Figure 2 illustrates how the high-resolution stable isotopes ($\delta^{18}\text{O}$, δD), smoothed ECM, chemical species and
10 their ratios are used in combination to decipher annual layer boundaries. All of these physico-chemical variables generally show a clear seasonality. The summer peak in water stable isotopes is obvious in most cases. Major ions such as nssSO_4 , $\text{SO}_4^-/\text{Na}^+$, NO_3^- generally help to distinguish ambiguous peaks in the isotopic record. SO_4^- is one of the oxidation products of Dimethyl Sulfide (DMS), a degradation product of DMSP which is synthesized by sea ice microorganisms (sympagic) as an antifreeze and osmotic regulator (e.g. Lepasseeur, 2013).
15 Both nssSO_4 and $R_{\text{Na}^+/\text{SO}_4^-}$ vary seasonally and are also strong indicators of volcanic eruptions. NO_3^- also shows a seasonal signal but the processes controlling its seasonality are not yet well understood (Wolff et al., 2008). For ECM, there is also a regular seasonal signal, but only to a depth of 80 m. The different age-depth profiles resulting from this counting procedure are presented in Figure 3. No ambiguity in layer counting is detectable above 62.38 m depth (i.e. 1933 A.D.). Between 249 and 269 annual cycles are identified between the reference
20 surface (2012 A.D.) and the bottom of the core, which is accordingly preliminarily dated to 1754 ± 10 A.D. before absolute dating.

3.1.2 Absolute dating

In order to further improve our annual layer estimates and the depth-age relationship, we have used the ECM signal (which is mainly inherited from the SO_4^- profile) to detect volcanic eruptions using a threshold from the
25 background signal of 2σ (Figure 4). The best depth-age match (corresponding to the closest age match at the base of the core) was obtained with the "oldest estimate", for which 12 peaks out of 33 could be assigned to known volcanic eruptions and one more from the chemistry alone (Krakatau - 1883). Following this absolute dating recalibration, the bottom of the core is dated to 1745. The year of deposition of each volcanic peak



allowed us to reduce the uncertainty of the depth-age relationship in the IC 12 core to ± 2 years. This is the precision usually associated with volcanic horizons, due to the time lapse between eruption and deposition (see sources in Table 1). The characteristics of these peaks are summarized in Table 1. The 1815 Tambora eruption has a clearly identifiable peak (Figure 4), which is expected from its high Volcanic Explosivity Index of 7 (Table 1) and its signal is detected up to two years after its eruption (e.g. Traufetter et al., 2004). Some eruptions, such as the 1762 Planchon-Peteroa eruption (assigned as unknown in Sigl et al., 2012) are recorded in both hemispheres (Sigl et al., 2012).

3.2 Snow accumulation rate history

Combining the annual layer thickness data set with the continuous IC12 density profile (published in Hubbard et al., 2013), we reconstructed the accumulation rate history at the summit of Derwael Ice Rise from 1745 to 2012. The cumulative thickness in w.e. is 91.8 m (Figure 5). Without correction for layer thinning, the mean annual layer thickness is 0.34 ± 0.003 m w.e., the lowest annual accumulation is 0.14 ± 0.05 m w.e. in 1834 and the highest is 1.05 ± 0.05 m w.e. in 1989 (Figure 6).

We applied two corrections: the piece-wise linear model (Dansgaard and Johnsen, 1969) and the fully linear model (Nye, 1963) (see Section 4.2) to investigate the influence of ice deformation on layer thickness, both techniques assuming a constant accumulation rate and a steady state. The piece-wise model approach cannot therefore be applied to the whole data set, since plotting annual layer thickness against depth in m w.e. reveals two trends with different slopes (Figure 5), suggesting an increase in accumulation rates. The transition occurs at ~ 49 m w.e., corresponding to 1900 A.D. Hypothesizing that, if accumulation rates have increased under the intensification of the hydrological cycle in response to the industrial revolution, we can consider the pre-1900 A.D. slope (0.003 a^{-1} , Figure 5) as representative of the rate of thinning associated with the constant long-term 'pre-industrial' rate of surface accumulation. We therefore used this strain rate value to correct annual layer thicknesses when applying the Dansgaard-Johnsen model.

Figure 6a shows the reconstructed history of annual accumulation rates at IC12 from 1745 to 2012, with associated error bars without ice deformation and with the two different ice-deformation models. As interannual variability is high, 11 years running means are also shown (thick lines in Figure 6a). As expected, the accumulation rate without ice deformation (blue lines in Figure 6a) is underestimated in the oldest part of the ice core as compared to the other two reconstructions taking ice deformation into account. The uncorrected curve shows a constant increase in accumulation, with multiple-step increases at ~ 1902 , 1955 and 1994 A.D. The constant increase in accumulation rates before 1902 attenuates with the correction based on the Nye approach for



taking deformation into account (green lines in Figure 6a and 6b) and becomes insignificant with the Dansgaard-Johnsen model (D-J, black lines in Figure 6a and 6b). However, all curves show a clear increasing trend in accumulation rates since the early 20th century.

Accumulation rates calculated on the basis of deformation corrections (Nye and D-J) and averaged over various
5 periods framed by volcanic horizons (e.g. Kaczmarska et al., 2004, Sigl et al. 2012; bold years in Table 1) are shown in Figure 6b and summarized in Table 2. The long term annual accumulation, starting from the oldest volcanic layer identified: 1768 to 2012, is between 0.39 and 0.46 m w.e. a⁻¹ depending on the correction applied (Table 2). The recent (1955-2012) accumulation rate is between 0.60 and 0.63 m w.e. a⁻¹ with, as expected, less
10 impact from the different deformation corrections. The sharpest increase occurs between the periods 1902-1955 and 1955-1992 (36% to 45% increase). With a 31 years running mean, the rate of accumulation change between 1902 and 1992 is 0.21 m w.e. a⁻¹ (data not shown).

Table 3 shows the detailed annual accumulation rates for the last 10 years for both corrections. The highest accumulation of the last 10 years occurred in 2009 and 2011, which belong to the 3% and 1% highest accumulation years of the whole record, respectively.

15 3.3 Relation to atmospheric and sea ice patterns

Figure 7 shows a summary of the output from the CESM as described in Section 2.5. In anomalously high-accumulation years (top panel), the sea ice coverage is very low (20-40 fewer days with sea-ice cover) in the Southern Ocean northeast of the ice core location, which is the prevalent source region of the atmospheric flow (Lenaerts et al., 2013). This is associated with higher near-surface temperatures (1-3 K), and a strengthening of
20 the low climatological low-pressure system (>1 hPa lower surface pressure), located offshore the ice core location (Lenaerts et al., 2013). In low-accumulation years (bottom panel), we see a reverse, albeit less strong, signal, with higher sea ice fraction, lower temperatures and higher core pressure of the low pressure system.

4 Discussion

4.1 Spatial and temporal variability

25 Our results show an increase in accumulation on the Derwael Ice Rise in coastal DML from 1955 onward. This confirms the studies that show a current increase in precipitation in coastal East Antarctica on the basis of satellite data and regional climate models (Davis et al., 2005, Lenaerts et al., 2012). Using a new glacial isostatic adjustment model, King et al. (2012) estimated that a 60 ± 13 Gt a⁻¹ mass increase of the East Antarctic Ice Sheet



- during the most recent period was concentrated along coastal regions, particularly in DML. However, until now, no change had been detected in ice cores from the area. Our study is the first in situ validation of a climate-related increase in coastal Antarctica precipitations which is expected to occur mainly in the peripheral areas at surface elevations below 2250 m (Krinner et al., 2007; Genthon et al., 2009).
- 5 However, not all of Antarctica would be expected to have the same accumulation trend. Figure 1 and Table A1 summarize results on accumulation trends from previous studies based on ice cores, extended with a few studies based on stake networks and radar. The colour of the site position on Figure 1 refers to the accumulation change at that site. The reference period refers to the last ~200 years, the recent period to the last ~50 years and the most recent period to the last ~20 years. The exact periods are given in Table A1.
- 10 Although the ISMASS Committee (2004) pointed out the importance of analysing coastal records, only 25 of the temporal records found in the literature concern ice cores drilled at the coast, and only 16 of them are located in DML. Only two of those records cover a period longer than 20 years: S100 (Kaczmarek et al., 2004) and B04 (Schlosser and Oerter, 2002). They both show a small decreasing trend (Figure 1).
- Most studies (69% of those comparing the last ~50 years with the last ~200 years) lack a significant trend (< 15 10% change). When we consider only the studies comparing the last 20 years to the last 200 years, the percentage lacking significant trend falls from 69% to 46%, for all Antarctica, but the trends revealed are both positive and negative. For example, Isaksson et al. (1996) found < 3% change at EPICA drilling site (Amundsenisen, DML) between 1865-1965 and 1966-1991. No trend was found on most inland and coastal sites (e.g. B31, S20) in DML, for the second part of the 20th century (Isaksson et al., 1999; Oerter et al. 1999, 2000; 20 Hofstede et al., 2004) or for the recent period (Fernandoy et al., 2010).
- A few studies (9% for the larger period and 18% for the shorter, more recent period) show a decrease of more than 10%. This is the case for several inland sites in DML (e.g. Anschutz et al., 2011), but also coastal sites in this region (Kaczmarek et al., 2004: S100; Isaksson & Melvold, 2002: Site H; Isaksson et al., 1999: S20; Isaksson et al., 1996: Site E; Isaksson et al., 1999: Site M).
- 25 Twenty-one percent of the studies record an increase of > 10% of accumulation rates from the middle of the 20th century, and 36% during the most recent period. In East Antarctica, increasing trends were only recorded at inland sites, e.g. in DML (Moore et al., 1991; Oerter et al., 2000), at South Pole Station (Mosley & Thompson, 1999), Dome C (Frezzotti et al., 2005), and around Dome A (Ren et al., 2010; Ding et al., 2011). Other increasing trends were found on the Antarctic Peninsula in coastal West Antarctica (Thomas et al., 2008; 30 Aristarain et al., 2004). For some sites, the increase only started during the most recent period (Site M: Karlof et al., 2005). The only other coastal site in East Antarctica potentially showing an increase in snow accumulation



rates is Talos Dome, where Frezzotti et al. (2013) reported a 19% decrease during the period 1966-1996 (compared to 1816-2001), while Stenni et al. (2002) reported an increase by 11% during 1992-1996 (compared to 1816-1996).

A pattern arises when we compare the low accumulation sites to the high accumulation sites (not all coastal), setting the threshold at 0.3 m w.e. a⁻¹, following Frezzotti et al. (2013) (Figure 8). The 11 sites above 0.3 m w.e. a⁻¹ show an average increase of accumulation of 33.8% between the last ~50 years and the reference period (last ~200 years), whereas the sites with lower accumulation show no trend (Figure 8a). This increase is more important (75%) if we compare the same reference period with the most recent period (last ~20 years) but this only covers two high accumulation sites, including IC12 (Figure 8b). Comparing the most recent period to the last ~50 years, the 12 high accumulation sites show an average increase of 10.1% (Figure 8c).

4.2 Sources of uncertainties

It is important to keep in mind that the trends, reported in this study (and others) have considerable uncertainties (Rupper et al., 2015). The accuracy of reconstruction of past snow accumulation rates depends on the dating exactness. Volcanic horizons are sometimes difficult to identify in coastal ice cores due to the ECM peaks associated with the presence of marine components. Also, given our vertical sampling resolution, the location of any single summer peak is only identifiable to a precision of 0.1 m. However, annual layer counting is easier than on inland sites, due to higher accumulation rates. Average accumulation rates on longer periods are preferred, since they are less affected by uncertainties than annual accumulation rates. These average estimates are also useful to reduce the influence of inter-annual variability.

Vertical strain rates are also a potential source of error. A companion paper will be dedicated to a more precise assessment of this factor using repeated borehole optical televiewer stratigraphy. However, the present study, by using a range of available strain rate models, shows that knowing the exact strain rates should not affect our main conclusions. Uncertainties are also influenced by the error on density and small scale variability in densification but these are assumed to be very small. For example, Callens et al. (submitted) used a semi-empirical model of firn compaction (Arthern et al., 2010) adjusting its parameters to fit the discrete measurements instead of using the best fit in Hubbard et al. (2013). Using the first model changes accumulation values by less than 2% (data not shown). Another source of possible error is the potential migration of the ice divide. Indeed, radar layers show accumulation asymmetry next to the Derwael ice Rise divide; if the divide migrated, it could have affected the change in accumulation. However, recent data indicate that there is a very low probability that such a migration occurred (Drews et al., 2015). Temporal variability at certain locations can



also be due to the presence of surface undulations up-glacier (e.g. Kaspari et al, 2004), but this is not the case for ice divides.

4.3 Causes of spatial and temporal variability

The increasing temporal trend in snow accumulation measured here and in ice cores from other areas and the spatial contrast observed could be the result of variable forcing: thermodynamic (temperature change), dynamic (change in atmospheric circulation) or both.

Increasing temperature increases the capacity of the air to hold vapour, generally enhancing precipitation. Oerter et al., (2000) showed a correlation between temperature and accumulation rates in DML. On longer timescales, using ice cores and models, Frieler et al., (2015) found a correlation between temperature and accumulation rates for the whole Antarctic continent. However, Altnau et al. (2015) found no correlation between snow accumulation and changes in ice $\delta^{18}\text{O}$ in coastal cores. They hypothesized that changes in synoptic circulation (cyclone activity) have more influence at the coast than thermodynamics alone. The increased frequency of blocking anticyclone and amplifying Rossby waves leads to the advection of moist air from the warmer middle and low latitudes (Schlosser et al., 2010; Frezzotti et al., 2013). This moisture transport is sometimes concentrated into “atmospheric rivers” of which two recent manifestations, in 2009 and 2011, have led to a positive anomaly in the net mass balance of East Antarctica (Shepherd et al., 2012; Boening et al., 2012) which was also observed in situ, at a local scale, next to the Belgian Princess Elisabeth base (72 °S, 21 °E) (Gorodetskaya et al., 2013; 2014). Such individual precipitation events can represent up to 50% of the annual accumulation (Schlosser et al., 2010; Lenaerts et al., 2013). These two highly variable accumulation events are also observed in our data as two notably higher than average accumulation years (2009 and 2011, Table 3). Our record puts these extreme events in an historical perspective, confirming that they are amongst the 1% to 3% highest accumulation years of the last two centuries, despite the fact that higher accumulation years exist in the recent part of record.

A change in climate modes could also partly explain recent changes in accumulation. The Southern Annular Mode (SAM) has shifted to a more positive phase during the last 50 years (Marshall, 2003). This has led to increasing cyclonic activity but also increasing wind speed and sublimation. Kaspari et al. (2004) also established a link between periods of increased accumulation and sustained El Niño events (negative Southern Oscillation Index (SOI) anomalies) in 1991-95 and 1940-42. We compared our detrended data set with SOI and SAM time series (KNMI, 2015) and found no correlation with either of those two indexes, yielding respective R^2 value of 0.0016 and 0.0026. In the detrended dataset, mean accumulation is indeed 5% higher during 1991-95



than the long-term average and 17% higher during 1940-42. However, high accumulation is also recorded during 1973-75 (19% higher than average) while that period is characterized by positive SOI values. Therefore, climate modes seem to have little influence on inter-annual variability of accumulation rates at IC12.

Small scale spatial variability in cyclonic activity and atmospheric rivers could explain why our results are different from others in the same region. Orography can greatly affect spatial variability in snow accumulation (Lenaerts et al., 2013). Highest snowfall and highest trends in predicted snowfall are expected in the escarpment zone, due to orographic uplift (Genthon et al., 2009). The main factor generating spatial variability, however, is commonly the wind; wind ablation represents one of the largest sources of uncertainty in modelling SMB. For example, in the escarpment area of DML, low and medium precipitation amounts can be entirely removed by the wind, while high precipitation events lead to net accumulation (Gorodetskaya et al., 2015). An enhanced wind speed coupled with an increase in accumulation could only increase SMB where the wind speed is low, while decreasing SMB in the windier areas (90% of the Antarctic surface (Frezzotti et al., 2004)). Frezzotti et al. (2013) suggested that snow accumulation has increased at low altitude sites and on the highest ridges due to more frequent anticyclone blocking events, but has decreased at intermediate altitudes due to stronger wind ablation in the escarpment areas. In DML however, Altnau et al. (2015) reported an accumulation increase on the plateau (coupled to an increase in $\delta^{18}\text{O}$) and a decrease on coastal sites, which they associated with a change in circulation patterns. Around Dome A, Ding et al. (2011) also reported an increase in accumulation rate in the inland area and a recent decrease towards the coast. Their explanation is that air masses may transfer moisture inland more easily due to climate warming.

A more recent study using a fully coupled climate model (Lenaerts et al., in press) suggests that DML is the region most susceptible to an increase in snowfall in a present and future warmer climate. The snowfall increase in the coastal regions is particularly attributed to loss of sea ice cover in the Southern Atlantic Ocean, which in turn enhances atmospheric moisture uptake by evaporation. This is further illustrated in Figure 7, which shows that extremely high accumulation years are associated with low sea ice cover. The longer exposure of open water leads to higher near-surface temperatures and enhances evaporation and moisture availability for ice sheet precipitation (Lenaerts et al., in press). Additionally, the low-pressure system, located offshore the ice core location (Lenaerts et al., 2013) is strengthened and invigorates meridional heat and moisture transport towards the ice sheet. The opposite is true for extremely low accumulation years.



5 Conclusions

A 120 m ice core was drilled on the divide of Derwael ice rise, and dated back to 1745 ± 2 A.D. using $\delta^{18}\text{O}$, δD , major ions where necessary, and volcanic horizons identified from ECM data. The mean accumulation at this site is 0.425 ± 0.035 m w.e. a^{-1} after corrections for densification and dynamic layer thinning. An increasing trend in accumulation rate is observed from 1955 onwards, as expected from climate models. The trends in accumulation observed in other records all over Antarctica are spatially highly variable. In coastal East Antarctica, our study is the only to show an increase in accumulation during the 20th and 21st centuries. Many studies point to a difference in the behaviour of coastal and inland sites, due to a combination of thermodynamics and dynamic processes. Our results of the CESM suggest that accumulation variability is largely explained by sea ice cover and atmospheric patterns. More studies are still clearly needed at other coastal sites in East Antarctica to determine how representative this result is.

Long time series are scarce in coastal East Antarctica. The divide of Derwael Ice Rise is a suitable drilling site for deep drilling. It has a high accumulation rate, and appropriate ice conditions (few thin ice layers) for paleoclimate reconstruction. With a 486 m ice thickness, drilling to the bedrock could reveal at least 2000 years of a reliable climate record with high resolution, a priority target of the International Partnership in Ice Core Science (IPICS, Steig et al., 2005).

Data Availability

Age-depth data and uncorrected accumulation rates are available online (doi:10.1594/PANGAEA.857574).

Acknowledgements

This paper forms a contribution to the Belgian Research Programme on the Antarctic (Belgian Federal Science Policy Office), Project SD/SA/06A Constraining ice mass changes in Antarctica (IceCon). The authors wish to thank the International Polar Foundation for logistic support in the field. MP is partly funded by a grant from Fonds David et Alice Van Buuren. JTML is funded by Utrecht University through its strategic theme Sustainability, sub-theme Water, Climate & Ecosystems, and the programme of the Netherlands Earth System Science Centre (NESSC), financially supported by the Ministry of Education, Culture and Science (OCW). Ph. C. thanks the Hercules Foundation (www.herculesstichting.be/) for financing the upgrade of the stable isotope laboratory. The research leading to these results has received funding from the European Research Council under



the European Community's Seventh Framework Programme (FP7/2007-2013) / ERC grant agreement 610055 as part of the Ice2Ice project. The authors also thank Irina Gorodetskaya for her helpful comments.

References

- Altnau, S., Schlosser, E., Isaksson, E., & Divine, D.: Climatic signals from 76 shallow firn cores in Dronning
5 Maud Land, East Antarctica. *The Cryosphere*, 9(3), 925-944, 2015.
- Anschütz, H., Müller K., Isaksson, E., McConnell, J. R., Fischer, H., Miller, H., Albert, M., and Winther, J.-G.: Revisiting sites of the South Pole Queen Maud Land Traverses in East Antarctica: accumulation data from shallow firn cores, *J. Geophys. Res.*, 114, D24106, doi:10.1029/2009JD012204, 2009.
- Anschütz, H., Sinisalo, A., Isaksson, E., McConnell, J. R., Hamran, S.-E., Bisiaux, M. M., Pasteris, D.,
10 Neumann, T. A., and Winther, J.-G.: Variation of accumulation rates over the last eight centuries on the East Antarctic Plateau derived from volcanic signals in ice cores, *J. Geophys. Res.*, 116, D20103, doi:10.1029/2011JD015753, 2011.
- Arthern, R. J., Vaughan, D. G., Rankin, A. M., Mulvaney, R., and Thomas, E. R.: In situ measurements of Antarctic snow compaction compared with predictions of models, *J. Geophys. Res.*, 115, F03011,
15 doi:10.1029/2009JF001306, 2010.
- Aristarain, A. J., Delmas, R. J., and Stievenard, M.: Ice-core study of the link between sea-salt aerosol, sea-ice cover and climate in the Antarctic Peninsula area, *Clim. Change*, 67, 63–86, 2004.
- Boening, C., Lebsack, M., Landerer, F., and Stephens, G.: Snowfall-driven mass change on the East Antarctic ice sheet, *Geophys. Res. Lett.*, 39, L21501, doi:10.1029/2012GL053316, 2012.
- 20 Bromwich, D. H., Nicolas, J. P., and Monaghan, A. J.: An assessment of precipitation changes over Antarctica and the Southern Ocean since 1989 in contemporary global reanalyses. *J. Clim.*, 24, 4189–4209, 2011.
- Callens, D., Drews, R., Witrant, E., Philippe, M., Pattyn, F.: Surface mass balance anomaly across an ice rise derived from internal reflection horizons through inverse modelling, *J. Glaciol.*, *in press*.
- Dansgaard, W. and Johnsen, S.: A flow model and a time scale for the ice core from Camp Century, Greenland,
25 *J. Glaciol.*, 8, 215-223, 1969.
- Davis, C. H., Li, Y., McConnell, J. R., Frey, M. M., & Hanna, E.: Snowfall-driven growth in East Antarctic Ice Sheet mitigates recent sea-level rise, *Science*, 308, 1898– 1901, 2005.



- Ding, M., Xiao, C., Li, Y., Ren, J., Hou, S., Jin, B., and Sun, B.: Spatial variability of surface mass balance along a traverse route from Zhongshan station to Dome A, Antarctica, *J. Glaciol.*, 57, 658–666, doi:10.3189/002214311797409820, 2011.
- Draws, R., Martin, C., Steinhage, D., & Eisen, O.: Characterizing the glaciological conditions at Halvfarryggen ice dome, Dronning Maud Land, Antarctica. *J. Glaciol.*, 59(213), 9–20, 2013.
- Draws, R., Matsuoka, K., Martín, C., Callens, D., Bergeot, N., and Pattyn, F.: Evolution of Derwael Ice Rise in Dronning Maud Land, Antarctica, over the last millennia. *J. Geophys. Res. Earth Surf.*, 120, 564–579. doi:10.1002/2014JF003246, 2015.
- Ekaykin, A. A., Lipenkov, V. Y., Kuzmina, I., Petit, J. R., Masson-Delmotte, V., and Johnsen, S. J.: The changes in isotope composition and accumulation of snow at Vostok station, East Antarctica, over the past 200 years, *Ann. Glaciol.*, 39, 569–575, 2004.
- Fernandoy, F., Meyer, H., Oerter, H., Wilhelms, F., Graf, W., and Schwander, J.: Temporal and spatial variation of stable-isotope ratios and accumulation rates in the hinterland of Neumayer station, East Antarctica, *J. Glaciol.*, 56, 673–687, 2010.
- Frezzotti, M., Pourchet, M., Flora, O., Gandolfi, S., Gay, M., Urbini, S., ... & Fily, M.: New estimations of precipitation and surface sublimation in East Antarctica from snow accumulation measurements, *Clim. Dyn.*, 23, 803 – 813, doi:10.1007/s00382-00004-00462-0038500803-00813, 2004.
- Frezzotti, M., Pourchet, M., Flora, O., Gandolfi, S., Gay, M., Urbini, S., Vincent, C., Becagli, S., Gagnani, R., Proposito, M., Severi, M., Traversi, R., Udasti, R., and Fily, M.: Spatial and temporal variability of snow accumulation in East Antarctica from traverse data, *J. Glaciol.*, 51, 113–124, 2005.
- Frezzotti, M., Urbini, S., Proposito, M., Scarchilli, C., and Gandolfi, S.: Spatial and temporal variability of surface mass balance near Talos Dome, East Antarctica, *J. Geophys. Res.*, 112, F02032, doi:10.1029/2006JF000638, 2007.
- Frieler, K., Clark, P. U., He, F., Buizert, C., Reese, R., Ligtenberg, S. R., ... & Levermann, A.: Consistent evidence of increasing Antarctic accumulation with warming. *Nature Climate Change*, 2015.
- Fujita, S., Holmlund, P., Andersson, I., Brown, I., Enomoto, H., Fujii, Y., Fujita, K., Fukui, K., Furukawa, T., Hansson, M., Hara, K., Hoshina, Y., Igarashi, M., Iizuka, Y., Imura, S., Ingvander, S., Karlin, T., Motoyama, H., Nakazawa, F., Oerter, H., Sjöberg, L. E., Sugiyama, S., Surdyk, S., Ström, J., Uemura, R., and Wilhelms, F.: Spatial and temporal variability of snow accumulation rate on the East Antarctic ice divide between Dome Fuji and EPICA DML, *The Cryosphere*, 5, 1057–1081, doi:10.5194/tc-5-1057-2011, 2011.



- Genthon, C., Krinner, G., & Castebrunet, H.: Antarctic precipitation and climate-change predictions: horizontal resolution and margin vs plateau issues. *Annals of Glaciology*, 50(50), 55-60, 2009.
- Gorodetskaya, I. V., Van Lipzig, N. P. M., Van den Broeke, M. R., Mangold, A., Boot, W., and Reijmer, C. H.: Meteorological regimes and accumulation patterns at Utsteinen, Dronning Maud Land, East Antarctica: Analysis of two contrasting years, *J. Geophys. Res.-Atmos.*, 118, 1700–1715, doi:10.1002/jgrd.50177, 2013.
- Gorodetskaya, I. V., Tsukernik, M., Claes, K., Ralph, M. F., Neff, W. D. and Van Lipzig, N. P. M.: The role of atmospheric rivers in anomalous snow accumulation in East Antarctica, *Geophys. Res. Lett.*, 41, 6199–6206, doi:10.1002/2014GL060881, 2014.
- Gorodetskaya, I. V., Kneifel, S., Maahn, M., Van Tricht, K., Thiery, W., Schween, J. H., ... & Van Lipzig, N. P. M.: Cloud and precipitation properties from ground-based remote-sensing instruments in East Antarctica. *The Cryosphere*, 9(1), 285-304, 2015.
- Hammer, C.U.: Acidity of polar ice cores in relation to absolute dating, past volcanism, and radio-echoes. *J. Glaciol.*, 25(93), 359–372, 1980.
- Hammer, C. U., Clausen, H. B., & Langway Jr, C. C.: Electrical conductivity method (ECM) stratigraphic dating of the Byrd Station ice core, Antarctica. *Annals of Glaciology*, 20, 115-120, 1994
- Hofstede, C. M., van de Wal, R. S. W., Kaspers, K. A., van den Broeke, M. R., Karl'of, L., Winther, J. G., Isaksson, E., Lappégard, G., Mulvaney, R., Oerther, H., and Wilhelms, F.: Firn accumulation records for the past 1000 years on the basis of dielectric profiling of six firn cores from Dronning Maud Land, Antarctica, *J. Glaciol.*, 50, 279–291, 2004.
- Hubbard, B., Roberson, S., Samyn, D., & Merton-Lyn, D.: Digital optical televueing of ice boreholes. *Journal of Glaciology*, 54(188), 823-830, 2008.
- Hubbard, B., Tison, J.-L., Philippe, M., Heene, B., Pattyn, F., Malone, T. and Freitag, J. J.: Ice shelf density reconstructed from optical televiewer borehole logging, *Geophys. Res. Lett.*, 40(22), 5882-5887, 2013.
- Igarashi, M., Nakai, Y., Motizuki, Y., Takahashi, K., Motoyama, H., and Makishima, K.: Dating of the Dome Fuji shallow ice core based on a record of volcanic eruptions from AD 1260 to AD 2001, *Polar Sci.*, 5, 411–420, doi:10.1016/j.polar.2011.08.001, 2011.
- Isaksson, E. and Melvold, K.: Trends and patterns in the recent accumulation and oxygen isotope in coastal Dronning Maud Land, Antarctica: interpretations from shallow ice cores, *Ann. Glaciol.*, 35, 175–180, 2002.
- Isaksson, E., Karlén, W., Gundestrup, N., Mayewski, P., Whitlow, S., and Twickler, M.: A century of accumulation and temperature changes in Dronning Maud Land, Antarctica, *J. Geophys. Res.*, 101, 7085–7094, 1996.



- Isaksson, E., van den Broeke, M. R., Winther, J.-G., Karlöf, L., Pinglot, J. F., and Gundestrup, N.: Accumulation and proxytemperature variability in Dronning Maud Land, Antarctica, determined from shallow firn cores, *Ann. Glaciol.*, 29, 17–22, 1999.
- ISMSS Committee: Recommendations for the collection and synthesis of Antarctic Ice Sheet mass balance data, *Global Planet. Change*, 42, 1–15, doi:10.1016/j.gloplacha.2003.11.008, 2004.
- Jiang, S., Cole-Dai, J., Li, Y., Ferris, D.G., Ma, H., An, C., Shi, G., and Sun, B.: A detailed 2840 year record of explosive volcanism in a shallow ice core from Dome A, East Antarctica, *J. Glaciol.*, 58, 65–75, doi:10.3189/2012JoG11J138, 2012.
- Kaczmarska, M., Isaksson, E., Karlöf, K., Winther, J-G, Kohler, J., Godtlielsen, F., Ringstad Olsen, L., Hofstede, C. M., van den Broeke, M. R., Van DeWal, R. S.W., and Gundestrup, N.: Accumulation variability derived from an ice core from coastal Dronning Maud Land, Antarctica, *Ann. Glaciol.*, 39, 339–345, 2004.
- Karlöf, L., Winther, J. G., Isaksson, E., Kohler, J., Pinglot, J. F., Wilhelms, F., ... & Wal, R. V. D.: A 1500 year record of accumulation at Amundsenisen western Dronning Maud Land, Antarctica, derived from electrical and radioactive measurements on a 120 m ice core. *J. Geophys. Res.: Atmospheres* (1984–2012), 105(D10), 12471–12483, 2000.
- Karlof, L., Isakson, E., Winther, J. G., Gundestrup, N., Meijer, H. A. J., Mulvaney, R., Pourcher, M., Hofstede, C., Lappegard, G., Petterson, R., van den Broecke, M. R., and van de Wal, R. S. W.: Accumulation variability over a small area in east Dronning Maud Land, Antarctica, as determined from shallow firn cores and snow pits: some implications for ice, *J. Glaciol.*, 51, 343– 352, doi:10.3189/172756505781829232, 2005.
- Kaspari, S., Mayewski, P. A., Dixon, D. A., Spikes, V. B., Sneed, S. B., Handley, M. J. and Hamilton, G. S.: Climate variability in west Antarctica derived from annual accumulation-rate records from ITASE firn/ice cores, *Ann. Glaciol.*, 39, 585–594, doi:10.3189/172756404781814447, 2004.
- King, M. A., Bingham, R. J., Moore, P., Whitehouse, P. L., Bentley, M. J., and Milne, G. A.: Lower satellite-gravimetry estimates of Antarctic sea-level contribution, *Nature*, 491, 586–589, doi:10.1038/nature11621, 2012.
- Kingslake, J., R. C. A. Hindmarsh, G. Aðalgeirsdóttir, H. Conway, H. F. J. Corr, F. Gillet-Chaulet, C. Martín, E. C. King, R. Mulvaney, and H. D. Pritchard: Full-depth englacial vertical ice sheet velocities measured using phase-sensitive radar, *J. Geophys. Res.: Earth Surface*, 119(12), 2604–2618, 2014.
- Kjaer, H.: Continuous chemistry in ice cores -Phosphorus, pH and the photolysis of humic like substances, University of Copenhagen, PhD thesis, 2014.
- KNMI Climate Explorer, SAM time series <http://www.nerc-bas.ac.uk/icd/gjma/sam.html>, WMO Regional Climate Centre, 2015a.



- KNMI Climate Explorer, SOI time series <http://www.cru.uea.ac.uk/cru/data/soi.htm>, WMO Regional Climate Centre, 2015b.
- Kohn, M. and Fujii Y.: Past 220 year bipolar volcanic signals: remarks on common features of their source volcanic eruptions. *Ann. Glaciol.*, 35, 217–223, 2002.
- 5 Krinner, G., Magand, O., Simmonds, I., Genthon, C., and Dufresne, J. L.: Simulated Antarctic precipitation and surface mass balance at the end of the 20th and 21st centuries, *Clim. Dynam.* 28, 215–230, doi:10.1007/s00382-006-0177-x, 2007.
- Langway, C.C., Osada, Jr K., Clausen, H. B., Hammer, C.U., Shoji, H. and Mitani, A.: New chemical stratigraphy over the last millennium for Byrd Station, Antarctica. *Tellus*, 46B(1), 40-51, 1994.
- 10 Lenaerts, J. T. M., van den Broeke, M. R., van den Berg, W. J., van Meijgaard, E., and Munneke, P. K.: A new, high resolution surface mass balance map of Antarctica (1979–2010) based on regional climate modeling, *Geophys. Res. Lett.*, 39, L04501, doi:10.1029/2011GL050713, 2012.
- Lenaerts, J. T. M., van Meijgaard, E., van den Broeke, M. R., Ligtenberg, S. R. M., Horwath, M., and Isaksson, E.: Recent snowfall anomalies in Dronning Maud Land, East Antarctica, in a historical and future climate
15 perspective, *Geophys. Res. Lett.*, 40, 1–5, doi : 10.1002/grl.50559, URL <http://doi.wiley.com/10.1002/grl.50559>, 2013.
- Lenaerts, J.T.M., Brownvan, J., den Broeke, M. R., Matsuoka, K., Drews, R., Callens, D., Philippe, M., Gorodetskaya, I., van Meijgaard, E., Reymer, C., Pattyn, F. and van Lipzig, N. P.: High variability of climate and surface mass balance induced by Antarctic ice rises. *J. Glaciol.*, 60(224): 1101, 2014.
- 20 Lenaerts, J. T. M., Vizcaino, M., Fyke, J., van Kampenhout, L., van den Broeke M. R.: Present-day and future Antarctic ice sheet climate and surface mass balance in the Community Earth System Model, *Clim. Dynam.*, *in press*.
- Levasseur, M.: Impact of Arctic meltdown on the microbial cycling of sulphur, *Nat. Geosci.*, 6, 691-700, 2013.
- Lliboutry, L. A.: A critical review of analytical approximate solutions for steady state velocities and temperature
25 in cold ice sheets, *Zeitschrift fur Gletscherkunde und Glazialgeologie Bd.*, 15, 135-148, 1979.
- Magand, O., Frezzotti, M., Pourchet, M., Stenni, B., Genoni, L., and Fily, M.: Climate variability along latitudinal and longitudinal transects in east Antarctica, *Ann. Glaciol.*, 39, 351–358, doi:10.3189/172756404781813961, 2004.
- Magand, O., Genthon, C., Fily, M., Krinner, G., Picard, G., Frezzotti, M., and Ekaykin, A. A.: An up-to-date
30 quality-controlled surface mass balance data set for the 90 –180E Antarctica sector and 1950–2005 period, *J. Geophys. Res.*, 112, D12106, doi:10.1029/2006JD007691, 2007.



- Marshall, G. J.: Trends in the southern annular mode from observations and reanalyses, *J. Climate*, 16, 4134–4143, 2003.
- Matsuoka, K., Hindmarsh, R. C., Moholdt, G., Bentley, M. J., Pritchard, H. D., Brown, J., ... & Hattermann, T.: Antarctic ice rises and rumples: their properties and significance for ice-sheet dynamics and evolution. *Earth-Sci. Rev.*, 150, 724–745, 2015.
- Monaghan, A. J., Bromwich, D. H., Fogt, R. L., Wang, S., Mayewski, P. A., Dixon, D. A., Ekaykin, A., Frezzotti, M., Goodwin, I., Isaksson, E., Kaspari, S. D., Morgan, V. I., Oerter, H., Van Ommen, T. D., van der Veen, C. J., and Wen, J.: Insignificant change in Antarctic snowfall since the International Geophysical Year, *Science*, 313, 827–831, doi:10.1126/science.1128243, 2006.
- Moore, J. C., Narita, H., and Maeno, N.: A continuous 770-year record of volcanic activity from East Antarctica, *J. Geophys. Res.*, 96, 17353–17359, 1991.
- Morgan, V. I., Goodwin, I. D., Etheridge, D. M., and Wookey, C. W.: Evidence for increased accumulation in Antarctica, *Nature*, 354, 58–60, 1991.
- Mosley-Thompson, E., Paskievitch, J. F., Gow, A. J., and Thompson, L. G.: Late 20th century increase in South Pole snow accumulation, *J. Geophys. Res.*, 104, 3877–3886, 1999.
- Mulvaney, R., Pasteur, E.C. and Peel, D.A.: The ratio of MSA to non sea-salt sulphate in Antarctic peninsula ice cores, *Tellus*, 44b, 293–303, 1992.
- Mulvaney, R., Oerter, H., Peel, D. A., Graf, W., Arrowsmith, C., Pasteur, E. C., Knight, B., Littot, G. C., and Miners, W. D: 1000-year ice core records from Berkner Island, Antarctic, *Ann. Glaciol.*, 35, 45–51, doi:10.3189/172756402781817176, 2002.
- Nishio, F., Furukawa, T., Hashida, G., Igarashi, M., Kameda, T., Kohno, M., Motoyama, H., Naoki, K., Satow, K., Suzuki, K., Morimasa, T., Toyama, Y., Yamada, T., and Watanabe, O.: Annual-layer determinations and 167 year records of past climate of H72 ice core in east Dronning Maud Land, Antarctica, *Ann. Glaciol.*, 35, 471–479, 2002.
- Nye, J.F.: Correction factor for accumulation measured by the thickness of the annual layers in an ice sheet. *J. Glaciol.*, 4(36), 785–788, 1963.
- Oerter, H., Graf, W., Wilhelms, F., Minikin, A., and Miller, H.: Accumulation studies on Amundsenisen, Dronning Maud Land, by means of tritium, DEP and stable isotope measurements: first results from the 1995/96 and 1996/97 field seasons, *Ann. Glaciol.*, 29, 1–9, doi:10.3189/172756499781820914, 1999.



- Oerter, H., Wilhelms, F., Jung-Rothenhausler, F., Goktas, F., Miller, H., Graf, W., and Sommer, S.: Accumulation rates in Dronning Maud Land as revealed by DEP measurements at shallow firn cores, *Ann. Glaciol.*, 30, 27–34, 2000.
- Parrenin, F., Dreyfus, G., Durand, G., Fujita, S., Gagliardini, O., Gillet, F., ... & Yoshida, N.: 1-D-ice flow
5 modelling at EPICA Dome C and Dome Fuji, East Antarctica. *Clim. Past*, 3(2), 243-259, 2007.
- Polvani, L. M., Waugh, D. W., Correa, G. J., & Son, S. W.: Stratospheric ozone depletion: The main driver of twentieth-century atmospheric circulation changes in the Southern Hemisphere. *J. Climate*, 24(3), 795-812, 2011.
- Raymond, C., Weertman, B., Thompson, L., Mosley-Thompson, E., Peel, D., and Mulvaney, R.: Geometry,
10 motion and balance of Dyer Plateau, Antarctica, *J. Glaciol.*, 42, 510–518, 1996.
- Ren, J., Li, C., Hou, S., Xiao, C., Qin, D., Li, Y., and Ding, M.: A 2680 year volcanic record from the DT-401 East Antarctic ice core, *J. Geophys. Res.*, 115, D11301, doi:10.1029/2009JD012892, 2010.
- Rignot, E., Velicogna, I., van den Broeke, M. R., Monaghan, A., and Lenaerts, J.: Acceleration of the contribution of the Greenland and Antarctic ice sheets to sea level rise, *Geophys. Res. Lett.*, 38, L05503,
15 doi:10.1029/2011GL046583, 2011.
- Roberts, J., Plummer, C., Vance, T., van Ommen, T., Moy, A., Poynter, S., ... & George, S.: A 2000-year annual record of snow accumulation rates for Law Dome, East Antarctica. *Clim. Past*, 11(5), 697-707, 2015.
- Rupper, S., Christensen, W. F., Bickmore, B. R., Burgener, L., Koenig, L. S., Koutnik, M. R., ... & Forster, R. R.: The effects of dating uncertainties on net accumulation estimates from firn cores. *J. Glaciol.*, 61(225), 163-
20 172, 2015.
- Ruth, U., Wagenbach, D., Mulvaney, R., Oerter, H., Graf, W., Pulz, H., and Littot, G.: Comprehensive 1000 year climate history from an intermediate depth ice core from the south dome of Berkner Island, Antarctica: methods, dating and first results, *Ann. Glaciol.*, 39, 146–154, 2004.
- Savitzky A., and Golay, M. J. E.: Smoothing and Differentiation of Data by Simplified Least Squares
25 Procedures. *Anal. Chem.*, 36 (8), pp 1627–1639, DOI: 10.1021/ac60214a047, 1964
- Schlosser, E. and Oerter, H.: Shallow firn cores from Neumayer, Ekströmisen, Antarctica: a comparison of accumulation rates and stable-isotope ratios. *Ann. Glaciol.*, 35, 91–96, 2002.
- Schlosser, E., Manning, K. W., Powers, J. G., Duda, M. G., Birnbaum, G., and Fujita, K.: Characteristics of high-precipitation events in Dronning Maud Land, Antarctica, *J. Geophys. Res.*, 115, D14107,
30 doi:10.1029/2009JD013410, 2010.



- Schlusser, E., Anshütz, H., Divine, D., Martma, T., Sinisalo, A., Altnau, S., and Isaksson, E.: Recent climate tendencies on an East Antarctic ice shelf inferred from a shallow firn core network, *J. Geophys. Res.*, 119, 6549–6562, 2014.
- Shepherd, A., Ivins, E. R., Geruo, A., Barletta, V. R., Bentley, M. J., Bettadpur, S., ... & Horwath, M.: A
5 reconciled estimate of ice-sheet mass balance. *Science*, 338(6111), 1183-1189, 2012.
- Sigl, M., McConnell, J. R., Layman, L., Maselli, O., McGwire, K., Pasteris, D., ... & Mulvaney, R.: A new bipolar ice core record of volcanism from WAIS Divide and NEEM and implications for climate forcing of the last 2000 years. *Journal of Geophysical Research: Atmospheres*, 118(3), 1151-1169, 2013.
- Steig, E., Fischer, H., Fisher, D., Frezzotti, M., Mulvaney, R., Taylor, K., Wolff, E.: The IPICS 2k Array: a
10 network of ice core climate and climate forcing records for the last two millennia, <http://www.pages-igbp.org/ipics/> IPICS (International Partnership in Ice Core Science, 2005).
- Stenni, B., Caprioli, R., Cimmino, L., Cremisini, C., Flora, O., Gragnani, R., Longinelli, A., Maggi, V., and Torcini, S.: 200 years of isotope and chemical records in a firn core from Hercules Neve, northern Victoria Land, Antarctica, *Ann. Glaciol.*, 29, 106–112, 1999.
- 15 Stenni, B., Proposito, M., Gragnani, R., Flora, O., Jouzel, J., Falourd, S., and Frezzotti, M.: Eight centuries of volcanic signal and climate change at Talos Dome (East Antarctica), *J. Geophys. Res.*, 107, 4076, doi:10.1029/2000JD000317, 2002.
- Sommer, S., Appenzeller, C., Röthlisberger, R., Hutterli, M. A., Stauffer, B., Wagenbach, D., Oerter, H., Wilhelms, F., Miller, H., and Mulvaney, R.: Glacio-chemical study spanning the past 2 kyr on three ice cores
20 from Dronning Maud Land, Antarctica, 1. Annually resolved accumulation rates, *J. Geophys. Res.*, 105, 29411–29421, 2000.
- Takahashi, H., Yokoyama, T., Igarashi, M., Motoyama, H., and Suzuki, K.: Resolution of environmental variation by detail analysis of YM85 shallow ice core in Antarctica, *Bull. Glaciol. Res.*, 27, 16–23, 2009.
- Thomas, E. R., Marshall, G. J., and McConnell, J. R.: A doubling in snow accumulation in the western Antarctic
25 Peninsula since 1850, *Geophys. Res. Lett.*, 35, L01706, doi:10.1029/2007GL032529, 2008.
- Trautetter, F., Oerter, H., Fischer, H., Weller, R., & Miller, H.: Spatio-temporal variability in volcanic sulphate deposition over the past 2 kyr in snow pits and firn cores from Amundsenisen, Antarctica. *Journal of Glaciology*, 50(168), 137-146, 2004.
- 35 van de Berg, W. J., van den Broeke, M. R., Reijmer, C. H., and van Meijgaard, E.: Reassessment of the Antarctic SMB using calibrated output of a regional atmospheric climate model, *J. Geophys. Res.*, 111, D11104, doi:10.1029/2005JD006495, 2006.



- van den Broeke, M., van de Berg, W. J., and van Meijgaard, E.: Snowfall in coastal West Antarctica much greater than previously assumed, *Geophys. Res. Lett.*, 33, L02505, doi:10.1029/2005GL025239, 2006.
- van Ommen, T. D. and Morgan, V.: Snowfall increase in coastal East Antarctica linked with southwest Western Australian drought, *Nat. Geosci.*, 3, 267–272, doi:10.1038/ngeo761, 2010.
- 5 Vaughan, D.G., Comiso, J.C., Allison, I., Carrasco, J., Kaser, G., Kwok, R., Mote, P., Murray, T., Paul, F., Ren, J., Rignot, E., Solomina, O., Steffen, K. and Zhang, T.: Observations: Cryosphere. In: *Climate Change 2013: The Physical Science Basis. Contribution of Working Group I to the Fifth Assessment Report of the Intergovernmental Panel on Climate Change* [Stocker, T.F., D. Qin, G.-K. Plattner, M. Tignor, S.K. Allen, J. Boschung, A. Nauels, Y. Xia, V. Bex and P.M. Midgley (eds.)]. Cambridge University Press, Cambridge, United Kingdom and New York, NY, USA, 2013.
- 10 Wolff, E. W., Jones, A. E., Bauguitte, S. B., & Salmon, R. A.: The interpretation of spikes and trends in concentration of nitrate in polar ice cores, based on evidence from snow and atmospheric measurements. *Atmospheric Chemistry and Physics*, 8(18), 5627-5634, 2008.
- Xiao, C., Mayewski, P. A., Qin, D., Li, Z., Zhang, M., and Yan, Y.: Sea level pressure variability over the southern Indian Ocean inferred from a glaciochemical record in Princess Elizabeth Land, east Antarctica, *J. Geophys. Res.*, 109, D16101, doi:10.1029/2003JD004065, 2004.
- 15 Zhang, M. J., Li, Z. Q., Xiao, C. D., Qin, D. H., Yang, H. A., Kang, J. C., & Li, J.: A continuous 250-year record of volcanic activity from Princess Elizabeth Land, East Antarctica. *Antarctic Science*, 14(01), 55-60, 2002.
- Zhang, M., Li, Z., Ren, J., Xiao, C., Qin, D., Kang, J., and Li, J.: 250 years of accumulation, oxygen isotope and chemical records in a firn core from Princess Elizabeth Land, East Antarctica, *J. Geogr. Sci.*, 16, 23–33, doi:10.1007/s11442-006-0103-5, 2006.
- 20



Tables

Table 1. Characteristics of the 12 volcanic peaks found in the IC12 core, and used to constrain the depth-age relationship to an uncertainty of ± 2 year. Bold years were used as reference for average accumulation calculations by period in Figure 6. Ref.: references: 1) Traufetter et al., 2004 and references therein ; 2) Kaczmarek et al., 2004 ; 3) Nishio et al., 2002 ; 4) Stenni et al., 2002 ; 5) Kohno and Fuji, 2002 ; 6) Zhang et al., 2002 ; 7) Moore et al., 1991 ; 8) Langway et al., 1994. *identified from ion chromatography.

Probable source volcano	Year of eruption	Year of deposition	VEI	Depth (m)	Difference between assigned age and year of deposition	Ref.
Unknown		2009		4.822		
Unknown		1995		20.01		
Pinatubo	1991	1992 ± 1	6	23.095	0	1
El Chichon	1982	1982 ± 1	4	33.63	-2	1
Unknown		1976		36.42		
Unknown		1973		38.58		
Unknown		1966		44.08		
Agung	1963	1964 ± 1	4	45.95	-1	1
Unknown		1961		47.15		
Carran-Los Venados	1955	1955 ± 1	4	50.79	0	2, 3
Unknown		1945		56.37		
Unknown		1940		59.24		
Unknown		1936		61.445		
Cerro Azul	1932	1932 ± 1	5	62.92	0	1
Unknown		1930		63.81		
Unknown		1922		67.26		
Unknown		1918		69.05		
Unknown		1916		69.82		
Unknown		1912		71.745		
Unknown		1908		73.49		
Santa Maria	1902	1902 ± 1	5	75.03	1	2, 4, 5
Unknown		1892		78.84		
Krakatau	1883	1884 ± 1	6	82.237*	0	1
Unknown		1844		94.98		
Coseguina	1835	1835 ± 1	5	97.34	0	1
Galunggung	1822	1822 ± 1	5	101.3	-1	2, 5, 6
Tambora	1815	1816 ± 1	7	102.4	2	1
Unknown	1809 ± 2	1809 ± 3	?	104	2	1
Cotopaxi	1768	1768 ± 1	4	115.3	-1	2, 7, 8
Planchon-Peteroa	1762	1762 ± 1	4	116.2	1	1
Unknown		1759		117.4		
Unknown		1750		119.2		
Unknown		1747		119.9		



Table 2. Average accumulation rates at IC12 for various time periods framed by volcanic horizons. The first year of each period is included, not the second (ex: 1768-2012: includes 1768, not 2012). Nye: correction for a linear decrease of annual layer thickness with depth. D-J: Corrected using a strain rate of 0.003 a^{-1} which is the slope of the annual layer thickness (in m w.e.) vs. depth relationship before 1900.

Period	Accumulation (m w. e. a^{-1}) (Nye)		Accumulation (m w. e. a^{-1}) (D-J)	
1768 - 2012	0.39	± 0.003	0.46	± 0.004
1992 - 2012	0.64	± 0.07	0.65	± 0.07
1955 - 1992	0.58	± 0.03	0.62	± 0.03
1902 - 1955	0.40	± 0.02	0.46	± 0.02
1884 - 1902	0.36	± 0.04	0.43	± 0.05
1816 - 1884	0.31	± 0.01	0.39	± 0.01
1768 - 1816	0.27	± 0.01	0.37	± 0.01
1768 - 1955	0.33	± 0.004	0.41	± 0.005
1955 - 2012	0.60	± 0.02	0.63	± 0.02

5

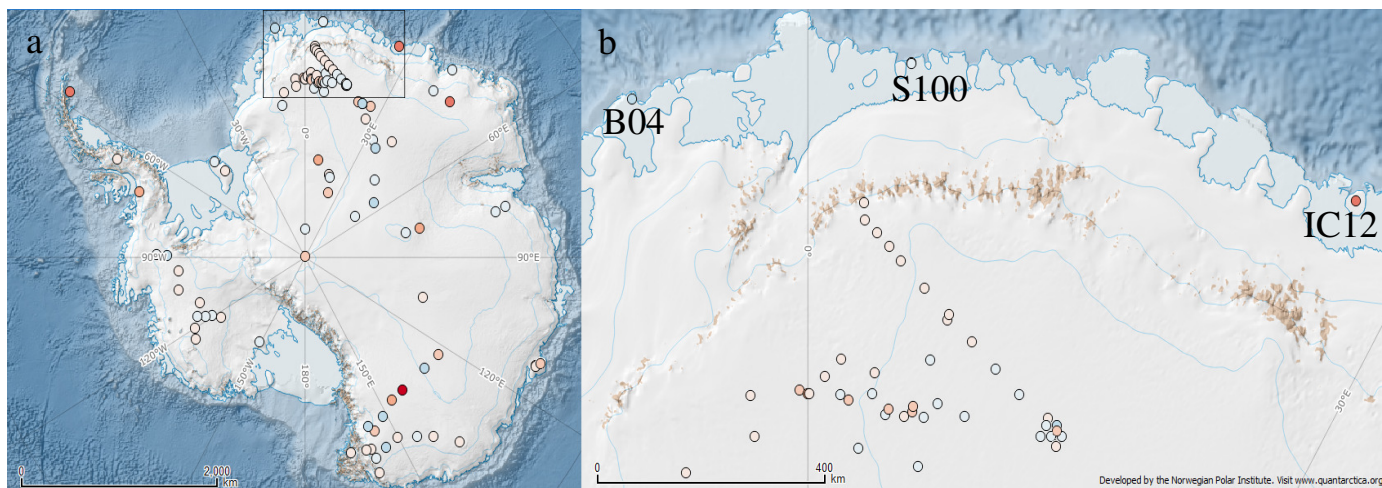


Table 3. Accumulation for the last 10 years from IC12 ice core. *See Table 2 legend and text for explanation
**not a full year

Year (A.D.)	Accumulation (m w.e. a ⁻¹) (Nye*)	Accumulation (m w.e. a ⁻¹) (D-J*)
2012**	0.482	0.482
2011	0.959	0.960
2010	0.632	0.634
2009	0.811	0.815
2008	0.642	0.646
2007	0.690	0.695
2006	0.653	0.658
2005	0.673	0.679
2004	0.658	0.666
2003	0.613	0.621



~1960-present vs ~1816-present



~1990-present vs ~1816 present

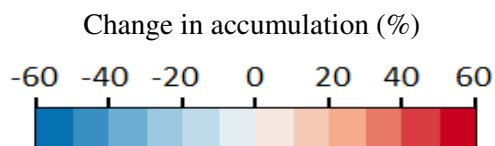
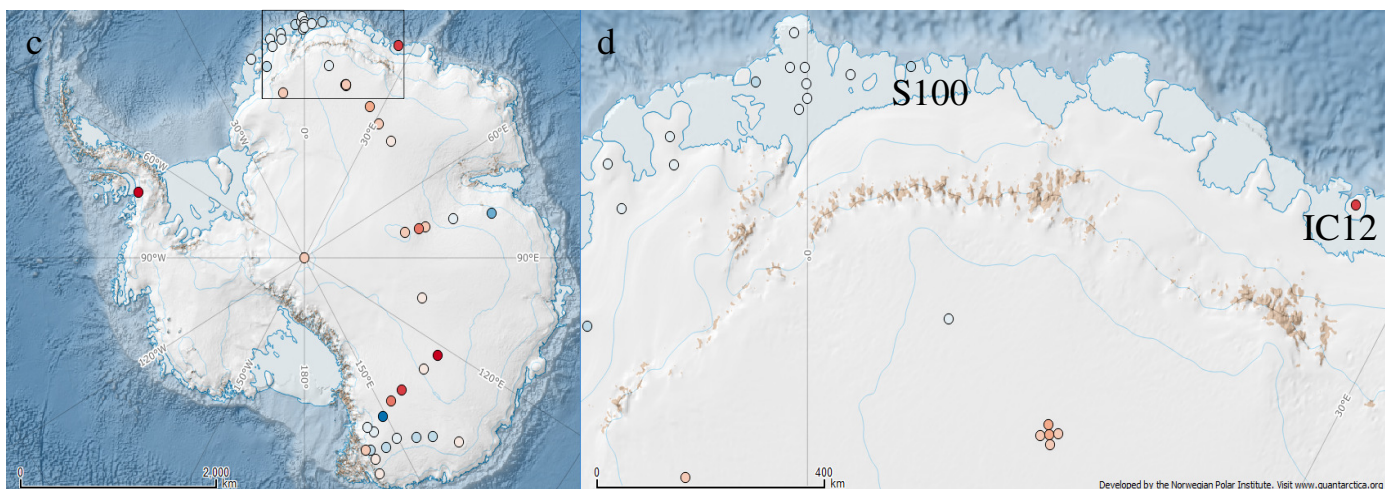


Figure 1: Location of IC12 and other ice cores referred to in the discussion. Change in Accumulation between ~1960-present average compared to ~1816-present average (a-b) and ~1990-present compared to 1816-present (c-d), see Table A1 for exact periods. Panels (b) and (d) are zoomed of the framed zone in panels (a) and (c).

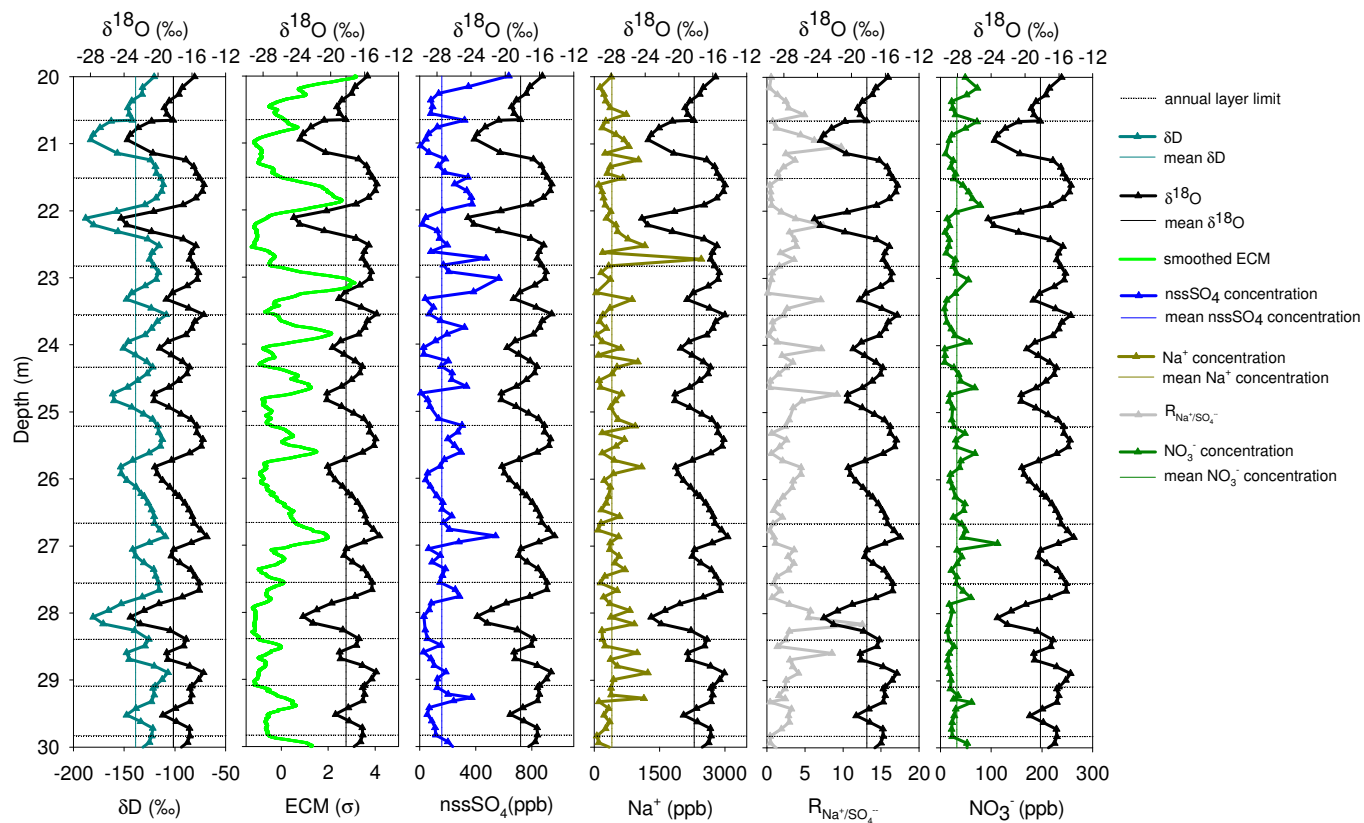


Figure 2. Variations in stable isotopes ($\delta^{18}\text{O}$, δD), smoothed ECM (running mean, 0.1 m), chemical species and their ratios used to constrain annual layer thickness in an example 10 m long section (20 - 30 m depth) of the IC12 ice core. Dashed horizontal lines indicate the annual layer limit (middle of the summer $\delta^{18}\text{O}$ peak).

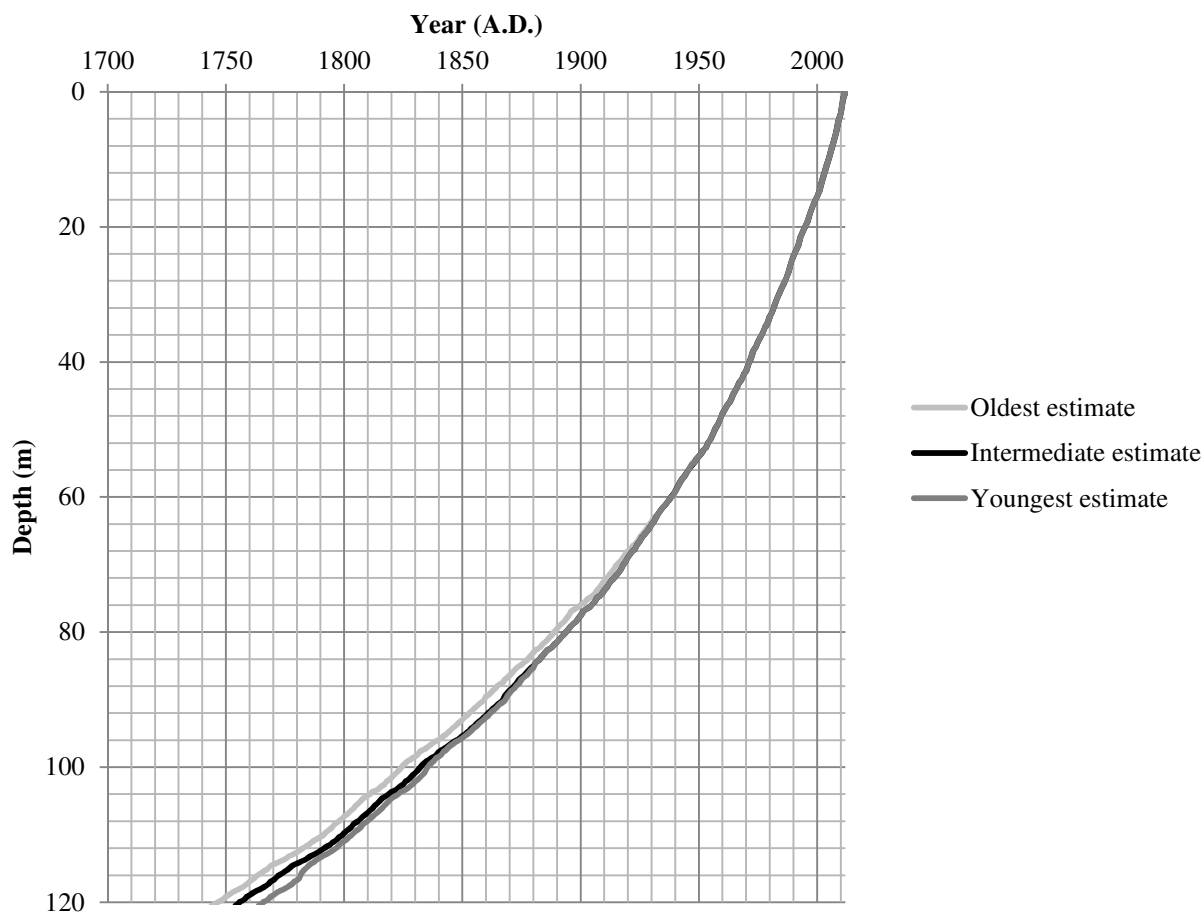


Figure 3. Age-depth relationships reconstructed from the relative dating process. Note that the approach results in no uncertainty above 62.38 m depth (year 1933). At 120 m depth, the uncertainty is ± 10 years.

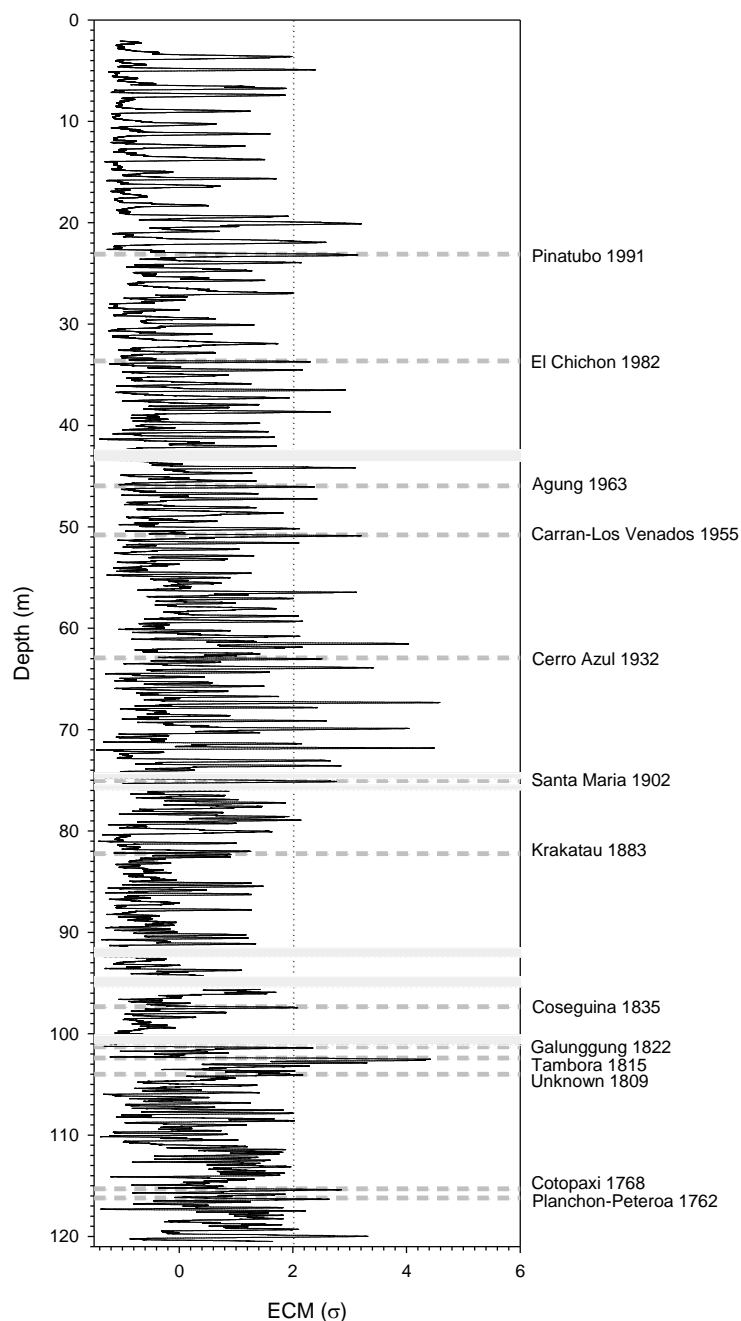


Figure 4. Continuous record of ECM (except for 6 measurement gaps shown as grey bands). Normalized conductivity (black line) is expressed as multiple of standard deviation (σ). The 2σ threshold is shown as a dotted vertical line, and identified volcanic peaks as dashed grey horizontal lines.

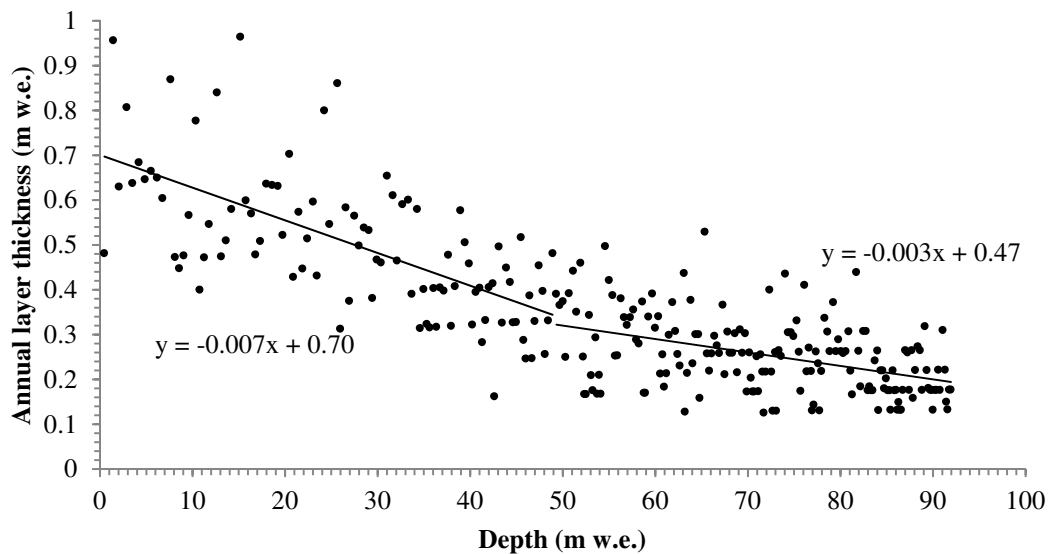


Figure 5. Annual layer thickness plotted against depth. The record is divided into two age/depth ranges, before and after 1900/49 m, for which best-fit straight lines are presented. We use the hypothesis that no temporal drift in annual accumulation existed prior to 1900 (see text for details).

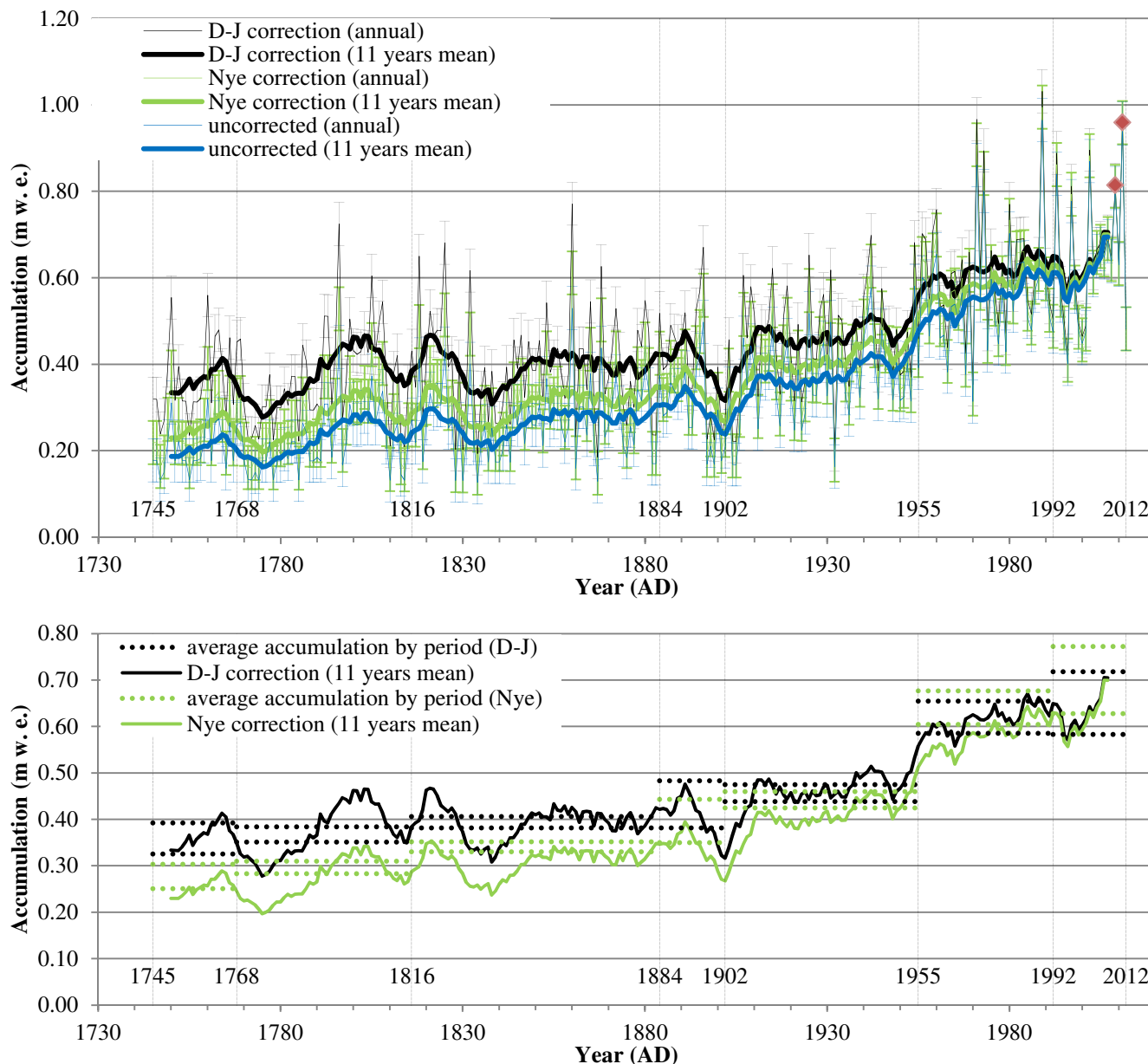


Figure 6. Accumulation rates at IC12. (a) Annual (thin lines with error bars) and average (11 years running mean, thick lines) accumulation rates. The blue lines show uncorrected annual layer thickness in m w.e. The red diamonds highlight years 2009 and 2011 discussed in the text (a-b) Corrected annual layer thicknesses are shown by green lines for the Nye approach and black lines for the Dansgaard and Johnsen approach (see text for details). (b) Dotted horizontal lines represent long-term accumulation (mean plus standard deviation and mean minus standard deviation) for various time periods bounded by specific volcanic eruption events (indicated by vertical lines and bold years).

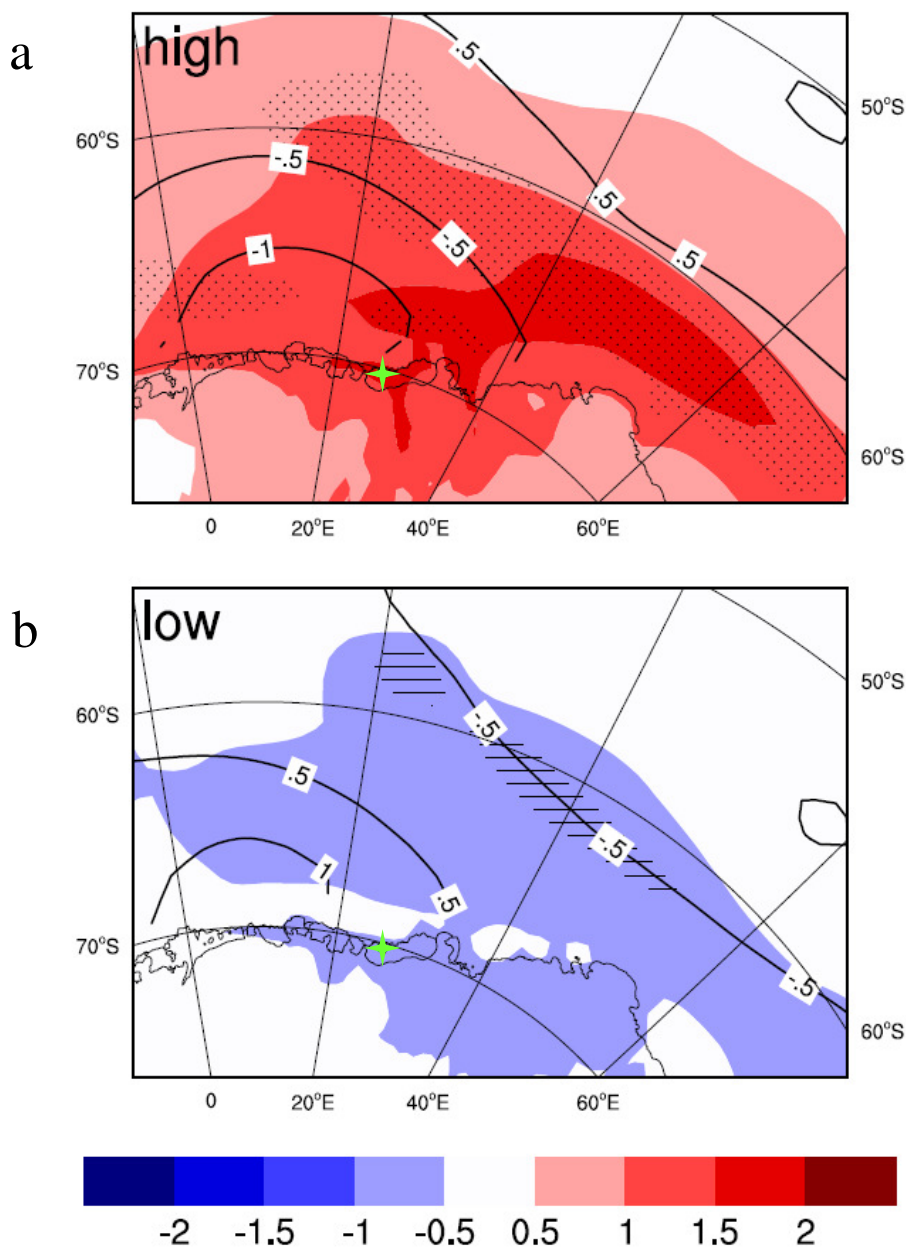


Figure 7. Large-scale atmospheric, ocean and sea-ice anomalies in (a) high-accumulation (10% highest) and (b) low-accumulation (10% lowest) years in the CESM historical time series (1850-2005). The colours show the annual mean near-surface temperature anomaly (in °C), the lines show the surface pressure anomaly (in hPa), and the stippled/hatched areas show the anomaly in sea-ice coverage (stippled areas are areas with >20 days less sea ice cover than the mean, hatched areas show areas with >20 days more sea ice than the mean). The green star shows the location of the ice core.

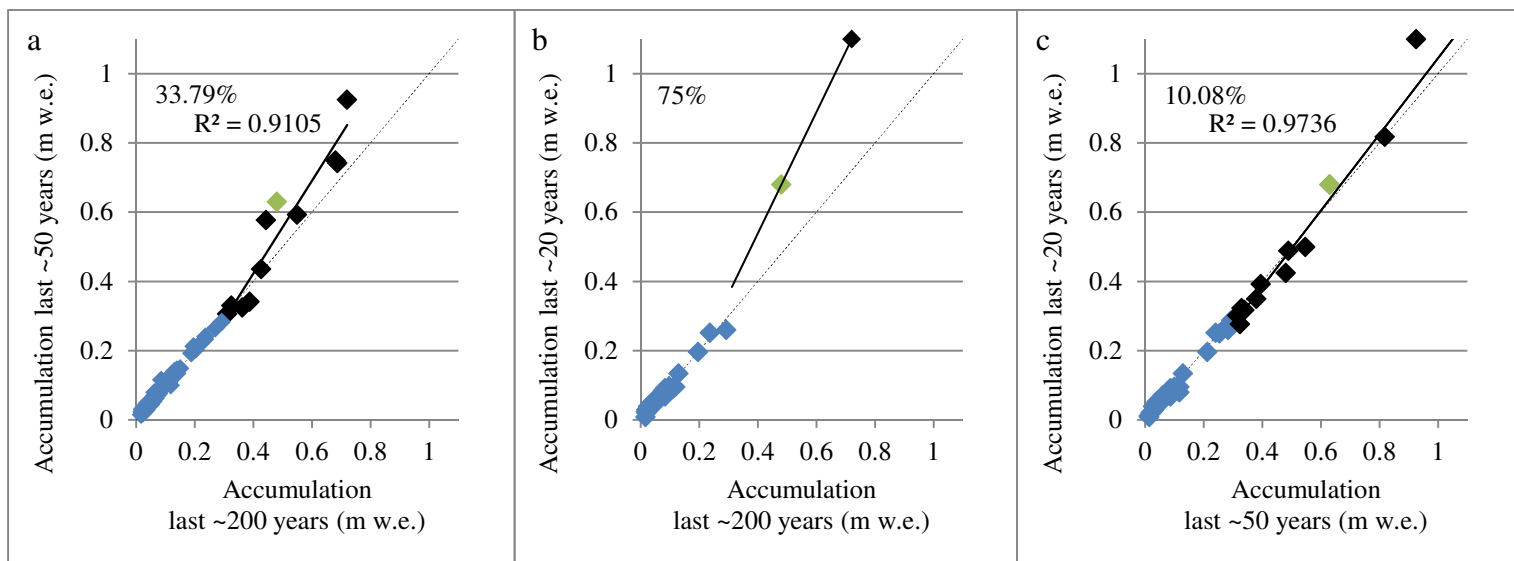


Figure 8. Comparison of SMB during (a) the last ~200 years and the last ~50 years (b) the last ~200 years and the last ~20 years, and (c) the last ~50 years and the last ~20 years. See Table A1 for exact periods. Sites above 0.3 m w.e. a⁻¹ are shown in black, except our study site, IC12 shown in green. Sites below 0.3 m w.e. a⁻¹ are shown in blue. The black lines show a linear regression through high accumulation sites. Increases in % between the periods compared are shown on the graph with R² value when relevant. The 1:1 slope (0% change) is shown as a dotted line.



Appendix A

Table A1. Sites information and snow accumulation values *no significant trend during the 20th century **short record: only recent periods are compared ***when only a stacked accumulation change is given, accumulation from individual ice cores are inferred from the stacked record as if it was the same trend for all ice cores. Ref : reference period. Numbers in italic are inferred from the trend given in the referenced paper

Site name	Latitude	Longitude	Elevation (m a.s.l.)	Reference period	Accumulation (10 ³ m w.e.) (kg m ² a ⁻¹)	Recent period	Accumulation (10 ³ m w.e.) (kg m ² a ⁻¹)	Most recent period	Accumulation (10 ³ m w.e.) (kg m ² a ⁻¹)	% change (50a - ref)	% change (20a - ref) except**	Method	Study	
Siple Dome	-81.6530	-148.9980	620	1890-1994	120	1922-1991	118			-1.67%		Ice core	Kaspari et al., 2004	
ITASE00-5	-77.6830	-123.9950	1828	1716-2000	140	1922-1991	141			0.71%		Ice core	Kaspari et al., 2004	
ITASE99-1	-80.6200	-122.6300	1350	1724-1998	139	1922-1991	146			5.04%		Ice core	Kaspari et al., 2004	
ITASE00-4	-78.0830	-120.0800	1697	1799-2000	189	1922-1991	193			2.12%		Ice core	Kaspari et al., 2004	
RIDS C	-80.0100	-119.4300	1530	1903-1995	112	1970-1995	108.35			-3.26%		Ice core	Kaspari et al., 2004	
RIDS B	-79.4600	-118.0500	1603	1922-1995	150	1970-1995	149.37			-0.42%		Ice core	Kaspari et al., 2004	
RIDS A	-78.7300	-116.3300	1740	1831-1995	235	1922-1991	234			-0.43%		Ice core	Kaspari et al., 2004	
ITASE00-1	-79.3830	-111.2390	1791	1653-2001	220	1922-1991	222			0.91%		Ice core	Kaspari et al., 2004	
ITASE01-2	-77.8430	-102.9100	1353	1890-2001	427	1922-1991	436			2.11%		Ice core	Kaspari et al., 2004	
ITASE01-3	-78.1200	-95.6460	1633	1859-2001	325	1922-1991	331			1.85%		Ice core	Kaspari et al., 2004	
ITASE01-5	-77.0590	-89.1370	1246	1780-2001	388	1922-1991	342			-11.86%		Ice core	Kaspari et al., 2004	
ITASE01-6	-76.0970	-89.0170	1232	**		1978-1999	392.6			-0.61%		Ice core	Kaspari et al., 2004	
Gomez	-73.5900	-70.3600	1400	1855-2006	720	1970s-2006	925	1997-2006	1100	28.47%	53%	Ice core	Thomas et al., 2008	
Dyer Plateau	-70.6700	-64.8900	2002	1790-1989	549	1969-1989	593			8.00%		Ice core	Raymond et al., 1996	
James Ross Island	-64.2200	-57.6800	1640	1847-1980	443	1964-1990	578			30.47%		Ice core	Aristarain et al., 2004	
R1	-78.3075	-46.2728	718	1816-1998	204	*	204			0.00%		Ice core	Mulvaney et al., 2002	
Berkner B25	-79.5700	-45.7200	890	1816-1956	131	1965-1994	141			7.63%		Ice core	Ruth et al., 2004	
A	-72.6500	-16.6333	60	**		1975-1989	380	1980-1989	350		-8%	Ice core	Isaksson & Melvold, 2002	
E	-73.6000	-12.4333	700	**		1932-1991	324	1980-1991	277		-15%	Ice core	Isaksson & Melvold, 2002; Isaksson et al., 1996	
B39	-71.4100	-9.9000	655	**		1935-2007	818	1987-2007	818		0.00%	Ice core	Fernandoy et al., 2010	
FB0704	-72.0600	-9.5600	760	**		1962-2007	489	1987-2007	489		0.00%	Ice core	Fernandoy et al., 2010	
BAS-depot	-77.0333	-9.5000	2176	1816-1997	71	1965-1997	71			0.00%		Ice core	Hofstede et al., 2004	
B04	-70.6200	-8.3700	35	1892-1981	362	±95 1960-1980	325			-10.22%		Ice core	Schlosser & Oerter, 2002	
CV	-76.0000	-8.0500	2400	1816-1997	62	1965-1997	68	±2 1992-1997	70	9.68%	13%	Ice core	Karlot et al., 2005	
B38	-71.1600	-6.7000	690	**		1960-2007	1257	1987-2007	1257		0.00%	Ice core	Fernandoy et al., 2010	
FB0702	-71.5700	-6.6700	539	**		1959-2007	547	1987-2007	500		-9%	Ice core	Fernandoy et al., 2010	
FB9816	-75.0000	-3.5037	2740	1800-1997	47	±17 1950-1997	51.5***			9.57%		Ice core	Oerter et al., 2000	
B31	-75.5800	-3.4300	2669	1816-1997	58.4	1966-1989	59.8			2.40%		Ice core	Oerter et al., 2000	
H	-70.5000	-2.4500	53	**		1953-1993	480	1980-1993	425		-11%	Ice core	Isaksson & Melvold, 2002	
NUS08-2	-87.8500	-1.8000	2583	1815-2007/8	67.4	±2.6 1963-2007/8	63.4	±4.2		-5.93%		Ice core	Anschutz et al., 2011	
S32	-70.3100	-0.8000	53	**		1995-2009	339	±36		-6%		Ice core	Schlosser et al., 2014	
G3	-69.8230	-0.6120	57	**		1993-2009	295	±29		-2%		Ice core	Schlosser et al., 2014	
FB9815	-74.9492	-0.5055	2840	1801-1997	59	±24 1950-1997	65***			10.17%		Ice core	Oerter et al., 2000	
G4	-70.9020	-0.4020	60	**		1983-2009	330	±21		-2%		Ice core	Schlosser et al., 2014	
M2	-70.3160	-0.1090	73	**		1981-2009	315	±22		-4%		Ice core	Schlosser et al., 2014	
G5	-70.5450	-0.0410	82	**		1983-2009	298	±21		-3%		Ice core	Schlosser et al., 2014	
K	-70.7500	0.0000	53	**		1954-1996	254	1980-1996	250		0%	Ice core	Isaksson & Melvold, 2002	
SPS	-90.0000	0.0000	2850	1816-1956	76.5	1965-1994	84.8	±3.3 1992-1997	84.5	±8.9	10.85%	10%	Ice core and poles	Mosley & Thompson, 1999
B32	-75.0023	0.0070	2882	1816-1997	63	1966-1997	80			26.98%		Ice core	Oerter et al., 2000	
EPICA DML	-75.0020	0.0680	2774	1915-2008	73	1964-2008	73.1	±1.7		0.14%		Firm core and radar	Fujita et al., 2011	
FB9808	-74.7507	0.9998	2860	1801-1997	68	±22 1950-1997	74.5***			9.56%		Ice core	Oerter et al., 2000	
FB9809	-74.4992	1.9608	2843	1801-1997	89	±29 1950-1997	97.5***			9.55%		Ice core	Oerter et al., 2000	
EPICA (Amundsenisen)	-75.0000	2.0000	2900	1865-1965	78	1966-1991	76			-2.56%		Ice core	Isaksson et al., 1996	
G8	-70.4100	2.0100	58	**		1991-2009	282	±26		273		Ice core	Schlosser et al., 2014	
FB9814	-75.0837	2.5017	2970	1801-1997	64	±21 1950-1997	71***			10.94%		Ice core	Oerter et al., 2000	
C	-72.2583	2.8911	2400	1955-1996	119	1965-1996	123			3.36%		Ice core	Isaksson et al., 1999	
D	-72.5083	3.0000	2610	1955-1996	112	1965-1996	116			3.57%		Ice core	Isaksson et al., 1999	
DML08	-75.7528	3.2828	2971	1919-96	60	±19 *	60			0.00%		Ice core	Oerter et al., 1999	
E	-72.6750	3.6628	2751	1955-1996	55	1965-1996	59			7.27%		Ice core	Isaksson et al., 1999	
DML02	-74.9683	3.9185	3027	1919-95	59	±14 *	59			0.00%		Ice core	Oerter et al., 1999	
FB9810	-74.6672	4.0017	2980	1801-1997	86	±29 1950-1997	94.5***			9.88%		Ice core	Oerter et al., 2000	
F	-72.8583	4.3514	2840	1955-1996	23	1965-1996	24			4.35%		Ice core	Isaksson et al., 1999	
S100	-70.2333	4.8000	48	1816-2000	292	1956-2000	284	1991-2000	260	±80	-2.74%	-11%	Ice core	Kaczmarek et al., 2004
S20	-70.2417	4.8111	63	1965-1996	271	1965-1996	265			-2.21%		Ice core	Isaksson et al., 1999	
FB0601	-75.2470	4.8440	3090	1915-2008	52	1964-2008	51.6	±1.2		-0.77%		Firm core and radar	Fujita et al., 2011	
FB9813	-75.1673	5.0033	3100	1816-1997	48	1950-1997	53***			10.42%		Ice core	Oerter et al., 2000	
G	-73.0417	5.0442	2929	1955-1996	28	1965-1996	30			7.14%		Ice core	Isaksson et al., 1999	
FB9804	-75.2503	6.0000	2630	1801-1997	50	±16 1950-1997	55***			10.00%		Ice core	Oerter et al., 2000	
H	-73.3917	6.4606	3074	1955-1996	44	1965-1996	46			4.55%		Ice core	Isaksson et al., 1999	



Site name	Latitude	Longitude	Elevation (m a.s.l.)	Reference period	Accumulation (10 ³ m w.e.) (kg m ² a ⁻¹)	Recent period	Accumulation (10 ³ m w.e.) (kg m ² a ⁻¹)	Most recent period	Accumulation (10 ³ m w.e.) (kg m ² a ⁻¹)	% change (50a - ref)	% change (20a - ref) except**	Method	Study		
B33	-75.1670	6.4985	3160	1816-1997	45.9	1966-1989	55			19.83%		Ice core	Oerter et al., 2000; Sommer et al., 2000		
FB9811	-75.0840	6.5000	3160	1801-1997	58	±16 1950-1997	64****			10.34%		Ice core	Oerter et al., 2000		
DML09	-75.9333	7.2130	3156	1897-1996	45	±12 *	45			0.00%		Ice core	Oerter et al., 1999		
DML10	-75.2167	7.2130	3364	1900-96	47	±11 *	47			0.00%		Ice core	Oerter et al., 1999		
DML04	-74.3990	7.2175	3179	1905-1996	53	±15 *	53			0.00%		Ice core	Oerter et al., 1999		
I	-73.8008	7.9406	3174	1955-1996	52	1965-1996	53			1.92%		Ice core	Isaksson et al., 1999		
NUS07-1	74.7200	7.9800	3174	1815-2007/8	52	±2 1963-2007/08	55.9	±3.9		7.50%		Ice core	Anschutz et al., 2009		
Site I	-73.7167	7.9833	3174	1815-2007	52	±1.3 1963-2007	56	±4.7	1991-2007	52	7.69%	0%	Ice core	Anschutz et al., 2009	
DML06	-75.0007	8.0053	3246	1899-1996	50	±14 *	50			0.00%		Ice core	Oerter et al., 1999		
NUS08-6	-81.7000	8.5700	2447	1815-2007/8	39.2	±1.5 1963-2007/8	49.2	±3.4		25.51%		Ice core	Anschutz et al., 2011		
J	-74.0417	9.4917	3268	1955-1996	44	1965-1996	45	±4		2.27%		Ice core	Isaksson et al., 1999		
FB0603	-75.1170	9.7240	3300	1915-2008	41	1964-2008	38	±0.9		-7.32%		Firm core and radar	Fujita et al., 2011		
K	-74.3583	11.1036	3341	1955-1996	45	1965-1996	41			-8.89%		Ice core	Isaksson et al., 1999		
L	-74.6417	12.7908	3406	1955-1996	45	1965-1996	41			-8.89%		Ice core	Isaksson et al., 1999		
A28	-74.8617	14.7420	3466	1915-2008	44	1964-2008	44.5	±1		1.14%		Firm core and radar	Fujita et al., 2011		
MC	-75.0112	14.8865	3470.4	1816-1884	40	1955-2000	39		1992-2000	46	-2.50%	15%	Ice core	Karhof et al., 2005	
MD	-74.9706	14.9567	3470.8	1816-1884	42	1955-2000	40		1992-2000	53	-4.76%	26%	Ice core	Karhof et al., 2005	
M	-75.0000	14.9964	3470	1816-1884	41	±0.7 1955-2000	41	±0.5	1992-2000	50	0.00%	22%	Ice core	Karhof et al., 2005	
M150	-74.9900	15.0000	3470	1816-1997	43	1965-1997	48.5			12.79%		Ice core	Hofstede et al., 2004		
M	-74.9917	15.0017	3453	1955-1965	51	1965-1996	45			-11.76%		Ice core	Isaksson et al., 1999		
MB	-75.0294	15.0435	3470.5	1816-1884	39	1955-2000	42		1992-2000	46	7.69%	18%	Ice core	Karhof et al., 2005	
MA	-74.9887	15.1134	3470.4	1816-1884	42	1955-2000	42		1992-2000	48	0.00%	14%	Ice core	Karhof et al., 2005	
NUS08-5	-82.6300	17.8700	2544	1815-2007/8	35	±0.8 1963-2007/8	37.6	±2.3		7.43%		Ice core	Anschutz et al., 2011		
NUS08-4	-82.8167	18.9000	2552	1815-2007/8	36.7	±0.9 1963-2007/8	36.1	±2.1		-1.63%		Ice core	Anschutz et al., 2011		
NUS08-3	-84.1300	22.0000	2625	1815-2007/8	40.1	±1 1963-2007/8	45.3	±3.1		12.97%		Ice core	Anschutz et al., 2011		
A35	-76.0660	22.4590	3586	1915-2008	35	1964-2008	39.2	±0.9		12.00%		Firm core and radar	Fujita et al., 2011		
NUS07-2	-76.0700	22.4700	3582	1815-2007/8	33	±0.7 1963-2007/8	28	±2		-15.15%		Ice core	Anschutz et al., 2011		
MP	-75.8880	25.8340	3661	1286-2008	33.1	±1.0 1964-2008	38.7	±0.9	1993-2008	41.9	±2.8	16.92%	27%	Firm core and radar	Fujita et al., 2011
NUS07-3	-77.0000	26.0500	3589	1815-2007/8	22	±0.5 1963-2007/8	23.7	±1.7		7.73%		Ice core	Anschutz et al., 2009		
IC12	-70.2458	26.3349	450	1816-2012	480	±1.0 1955-2012	630	±2.0	1992-2012	680	±7.0	31.25%	42%	Ice core	This paper
DK190	-76.7940	31.9000	3741	1286-2008	28.7	±0.9			1993-2008	34.1	±2.3	19%	Firm core and radar	Fujita et al., 2011	
NUS07-4	-78.2167	32.8500	3595	1815-2007/8	19	±0.5 1963-2007/8	17.5	±1.2		-7.89%		Ice core	Anschutz et al., 2009		
NUS07-5	-78.6500	35.6300	3619	1815-2007/8	24	±0.5 1963-2007/8	20.1	±1.4		-16.25%		Ice core	Anschutz et al., 2011		
DF	-77.3170	39.7030	3810	1816-2001	26.3	1964-2008	28.8	±0.7	1995-2006	27.3	±0.4	9.51%	4%	Ice core	Igarashi et al., 2011
YM85	-71.5800	40.6300	2246	1816-2002	140	1965-2002	135			-3.57%		Ice core	Takahashi et al., 2009		
H72	-69.2047	41.0906	1214	1831-1998	311	1973-1998	307			-1.29%		Ice core and poles	Nishio et al., 2002		
NUS07-6	-80.7833	44.8500	3672	1815-2007/8	22	1902-2007/8	21			-4.55%		Ice core	Anschutz et al., 2009		
G15	-71.2000	45.9800	2544	1816-1964	86	1964-1984	116			34.88%		Ice core	Moore et al., 1991		
NUS07-8	-84.1833	53.5333	3452	1815-2007/8	32	±1.2 1963-2007/8	30	±2.1		-6.25%		Ice core	Anschutz et al., 2009		
NUS07-7	-82.0700	54.5500	3725	1815-2007/8	29.4	±0.6 1963-2007/8	26.1	±1.9		-11.22%		Ice core	Anschutz et al., 2011		
DT217	-75.7167	76.8333	2800	**		1998-2008	12	±1.72	2005-2008	12		0%	Stake arrays	Ding et al., 2011	
DT364	-78.3333	77.0000	3380	**		1999-2008	62	±0.14	2005-2008	72		16%	Stake arrays	Ding et al., 2011	
DT401	-79.0200	77.0000	3760	1816-1999	19	1963-1999	24		1999-2005	25	±16	26.32%	32%	Ice core	Ren et al., 2010; Ding et al., 2011a
DT001	-70.8300	77.0700	2325	1810-1959	131	1959-1996	131			0.00%		Ice core	Zhang et al., 2006		
Dome A	-80.3667	77.3500	4093	**		2005-2008	19	±0.25	2008-2009	21		11%	Stake arrays	Ding et al., 2011	
DomeA	-80.3600	77.3600	4092	1815-1998	23	1963-1998	23			0.00%		Ice core	Jiang et al., 2012		
LGB65	-71.8500	77.9200	1850	1815-1996	131	1960-1996	131			0.00%		Ice core	Xiao et al., 2004		
DT008	-72.1667	77.9333	2390	**		1998-2008	118	±0.30	2005-2008	80		-32%	Stake arrays	Ding et al., 2011	
VOSTOK	-78.4500	106.8300	3488	1816-2010	20.6	±0.3 1955-2010	21.5	±0.5	1958-2010	20.8		4.37%	1%	Snow pits and poles	Ekaykin et al., 2004
DSS	-66.7697	112.8069	1370	1816-2000	680	1970-2009	750			10.29%		Ice core	Roberts et al., 2015		
LAW DOME	-66.7700	112.9800	1370	1816-1966	687	1966-2005	742			8.01%		Ice core	Morgan et al., 1991; van Ommen & Morgan, 2010		
DomeC	-75.1200	123.3100	3233	1816-1998	25.3	1965-1998	28.3		1996-1998	39		11.86%	54%	Ice core and poles	Frezzotti et al., 2005
D6 A	-75.4400	129.8100	3027	1816-1998	36	±1.8 1966-1998	29	±1.4	1998-2002	39		-19.44%	8%	Ice core and poles	Frezzotti et al., 2005
D66	-68.9400	136.9400	2333	1966-1864	196	1965-2001	213	±13	2001-2003	197		8.67%	1%	Ice core and poles	Magand et al., 2004; Frezzotti et al., 2013
D2 A	-75.6200	140.6300	2479	1816-1998	20	±1.0 1966-1998	31	±1.6	1998-2002	30		55.00%	50%	Ice core and poles	Frezzotti et al., 2005
GV1	-70.8700	141.3800	2244	1816-2001	114	1965-2001	117	±7	2001-2003	96		2.63%	-16%	Ice core and poles	Magand et al., 2004; Frezzotti et al., 2013
GV2	-71.7100	145.2600	2143	1816-2001	112	1965-2001	112	±7	2001-2003	92		0.00%	-18%	Ice core and poles	Magand et al., 2004; Frezzotti et al., 2013
MdPtA	-75.5300	145.8600	2454	1816-1998	36	±1.8 1966-1998	45	±2.7	1998-2010	47		25.00%	31%	Ice core and poles	Frezzotti et al., 2005



Site name	Latitude	Longitude	Elevation (m a.s.l.)	Reference period	Accumulation (10 ³ m w.e.) (kg m ² a ⁻¹)	Recent period	Accumulation (10 ³ m w.e.) (kg m ² a ⁻¹)	Most recent period	Accumulation (10 ³ m w.e.) (kg m ² a ⁻¹)	% change (50a - ref)	% change (20a - ref) except**	Method	Study		
GV3	-72.6300	150.1700	2137	1816-2001	81	1965-2001	84	±5	2001-2003	73	3.70%	-10%	Ice core and poles	Magand et al., 2004; Frezzotti et al., 2013	
M2 A	-74.8000	151.2700	2278	1816-1998	17	±0.8	1966-1998	15	±7.5	1998-2002	8.5	-11.76%	-50%	Ice core and poles	Frezzotti et al., 2005
GV4	-72.3900	154.4800	2126	1816-2001	119		1965-2001	100	±6	2001-2003	96	-15.97%	-19%	Ice core and poles	Magand et al., 2004; Frezzotti et al., 2013
31DPT A	-74.0300	155.9600	2069	1816-1998	98	±4.9	1966-1998	112	±5.6	1998-2002	98	14.29%	0%	Ice core and poles	Frezzotti et al., 2005
GPS2A	-74.6400	157.5020	1804	1816-1998	60	±3.0	1966-1998	54	±2.7	1993-2000	55	-10.00%	-8%	Ice core and poles	Frezzotti et al., 2005
GV5	-71.8900	158.5400	2184	1816-2001	129		1965-2001	129	±7	2001-2004	135	0.00%	5%	Ice core and poles	Magand et al., 2004; Frezzotti et al., 2007
GV7	-70.6800	158.8600	1947	1854-2001	237		1965-2001	241	±13	2001-2004	252	1.69%	6%	Ice core and poles	Magand et al., 2004; Frezzotti et al., 2007
Talos Dome	-72.7700	159.0800	2316	1816-2001	83.6		1966-1996	86.6		2001-2010	68	3.59%	-19%	Ice core and poles	Magand et al., 2004; Frezzotti et al., 2007; 2013
Talos Dome	-72.8000	159.1000	2246	1816-1996	83.6		1966-1996	86.6		1992-1996	92.5	3.59%	11%	Ice core	Stenni et al., 2002
Hercules Neve	-73.1000	165.4000	2960	1816-1966	118		1966-1992	129				9.32%		Ice core	Stenni et al., 1999